

QCD-like theories at nonzero temperature and density

Tian Zhang,^a Tomáš Brauner^{a*} and Dirk H. Rischke^{a,b}

^a*Institute for Theoretical Physics, Goethe University, Frankfurt am Main, Germany*

^b*Frankfurt Institute for Advanced Studies, Frankfurt am Main, Germany*

E-mail: tzhang@th.physik.uni-frankfurt.de,

brauner@th.physik.uni-frankfurt.de, drischke@th.physik.uni-frankfurt.de

ABSTRACT: We investigate the properties of hot and/or dense matter in QCD-like theories with quarks in a (pseudo)real representation of the gauge group using the Nambu–Jona-Lasinio model. The gauge dynamics is modeled using a simple lattice spin model with nearest-neighbor interactions. We first keep our discussion as general as possible, and only later focus on theories with adjoint quarks of two or three colors. Calculating the phase diagram in the plane of temperature and quark chemical potential, it is qualitatively confirmed that the critical temperature of the chiral phase transition is much higher than the deconfinement transition temperature. At a chemical potential equal to half of the diquark mass in the vacuum, a diquark Bose–Einstein condensation (BEC) phase transition occurs. In the two-color case, a Ginzburg–Landau expansion is used to study the tetracritical behavior around the intersection point of the deconfinement and BEC transition lines, which are both of second order. We obtain a compact expression for the expectation value of the Polyakov loop in an arbitrary representation of the gauge group (for any number of colors), which allows us to study Casimir scaling at both nonzero temperature and chemical potential.

KEYWORDS: QCD, Confinement, Chiral Lagrangians, Spontaneous Symmetry Breaking.

*On leave from Department of Theoretical Physics, Nuclear Physics Institute ASCR, Řež, Czech Republic.

Contents

1. Introduction	1
2. Model setup	3
2.1 Gauge sector	3
2.2 Quark sector	6
2.3 Mean-field approximation	8
2.4 Parameter fixing in the quark sector	9
3. Two colors	10
3.1 Phase diagram	11
3.2 Tetracritical point	13
3.3 Casimir scaling	15
4. Three colors	17
4.1 Phase diagram	18
4.2 Casimir scaling	19
5. Conclusions	20
A. Fierz transformation of the current–current interaction	22
B. Gauge group averaging with continuum quarks	22
C. Group integration for $SU(N)$	25

1. Introduction

Quantum chromodynamics (QCD) is accepted as the theory for strongly interacting matter. However, due to the strong coupling, perturbative treatments fail at an energy scale of the order of Λ_{QCD} , resulting in the fact that the structure of the QCD vacuum is still far from being well understood. The same is true of the QCD phase diagram where, due to the formidable sign problem, standard Monte-Carlo techniques based on importance sampling cannot be used at nonzero quark chemical potential.

In order to get deeper insight into the behavior of dense quark matter, several QCD-like theories have been proposed, including QCD with an imaginary chemical potential [1], at nonzero isospin density [2], two-color QCD with fundamental quarks [3], and any-color QCD with adjoint quarks [4]. All these theories share the pleasing feature that they are

free of the sign problem, which makes them possible to be simulated on the lattice from first principles.

In the present paper we focus on two wide classes of QCD-like theories: those with nonzero *baryon* chemical potential and quarks in a *real* or *pseudoreal* representation of the gauge group. For the sake of brevity, they will be henceforth referred to as *type-I* and *type-II QCD-like theories*, respectively (see, e.g., Refs. [5, 6] for applications of these theories in another, electroweak, sector of the standard model of elementary particles). The typical examples are QCD with adjoint quarks of two (aQC₂D) or three (aQCD) colors for type I, and two-color QCD with fundamental quarks (QC₂D) for type II. While the effective Nambu–Jona-Lasinio (NJL) model description for the latter was worked out in Refs. [7, 8, 9, 10, 11], the model Lagrangian for type-I theories is, as far as we know for the first time, constructed here.¹ Due to the (pseudo)reality of the quark representation of the gauge group, all these theories have several remarkable differences as compared to ordinary QCD, besides the absence of the sign problem itself.

First, with N_f massless quark flavors, the global flavor symmetry is $SU(2N_f)$ rather than the usual chiral group $SU(N_f)_L \times SU(N_f)_R \times U(1)_B$. The reason is that the charge-conjugated quark field $(\psi_R)^\mathcal{C}$ (charge conjugation being defined as $\psi^\mathcal{C} = C\bar{\psi}^T$) which is a left-handed spinor transforms in the same way as the left-handed quark ψ_L under both color and Lorentz transformations, so it is allowed to transform them into each other while keeping the color symmetry intact. This means that the multiplets of states in the spectrum will contain modes of different baryon number. In particular, apart from the pions the Nambu–Goldstone (NG) bosons of the spontaneously broken flavor symmetry will also include diquarks. These light diquarks are colorless bosons carrying baryon charge, and hence at low temperature and sufficiently high chemical potential, they will undergo Bose–Einstein condensation (BEC).

Second, in case of quarks in a real (such as the adjoint) representation, the Z_{N_c} center symmetry remains intact in the presence of dynamical quarks. This leads to a well-defined deconfinement phase transition, accompanied by spontaneous center symmetry breaking, instead of a crossover as in QCD [13]. The associated order parameter is the expectation value of the Polyakov loop. For the two- and three-color cases investigated in this paper, the deconfinement transition is of second and of first order, respectively.

Since the BEC and deconfinement phase transitions are both well-defined, being associated with exact symmetries even in the presence of massive dynamical quarks, aQC₂D exhibits a rather unusual critical behavior in the vicinity of the tetracritical point where the two second-order transition lines cross each other [14]. In (three-color) aQCD the deconfinement transition is of first order. As a consequence the second-order BEC critical line is interrupted around the deconfinement transition, meeting the deconfinement line at two tricritical points. This general expectation is confirmed by our explicit model calculation.

To model the gauge sector, we use a simple lattice spin model with nearest-neighbor interaction, inspired by the strong-coupling expansion [15, 16, 17, 18, 19, 20]. This is then coupled to continuum quarks in a fashion similar to the Polyakov-loop NJL (PNJL)

¹A Polyakov loop NJL-type model for adjoint fermions was already worked out in Ref. [12], but the quark sector of their Lagrangian does not have the $SU(2N_f)$ symmetry of the underlying gauge theory.

model [20, 21, 22, 23, 24, 25]. As an effective model, the NJL model successfully describes chiral symmetry breaking and pairing of quarks. But since it contains no dynamical gluons, the confinement feature is missing. In order to account for confinement at least in a heuristic way, one adds to the thermodynamic potential an effective potential for the Polyakov loop, adjusted to reproduce the thermodynamic observables in the pure gauge theory. The Polyakov loop is represented by a constant temporal background gluon field which in turn couples to the quarks [21]. The parameters of the PNJL model are fixed separately in the pure gauge and chiral quark sectors. The successful qualitative reproduction of the coincidence of the deconfinement and chiral restoration temperatures, T_d and T_χ , in QCD is then one of the great virtues of the PNJL model. On the other hand, aQCD is very different. First, $T_d \ll T_\chi$, resulting in a broad range of temperatures exhibiting deconfined, but still chirally broken matter [26, 27, 28] (see also Refs. [12, 29] for related theories with periodic boundary conditions for quarks). Second, T_d does not change much compared to the pure gauge theory when quarks are coupled in, because adjoint quarks carry zero center charge. We confirm these features in our results.

The paper is organized as follows. In Sec. 2 we introduce our model, working out separately the actions in the gauge and quark sectors. The gauge part is well known from literature, and we therefore just elaborate on the Weiss mean-field approximation used in this paper. In the quark part we deal with the task to construct an interaction Lagrangian with $SU(2N_f)$ flavor symmetry. While this was previously achieved for QC_2D and actually applies equally well to all type-II theories, here we construct analogously a model Lagrangian for type-I theories. Section 3 is devoted to two-color QCD. We study the phase diagram of a QC_2D and derive the Ginzburg–Landau (GL) theory that governs the behavior of the system near the tetracritical point. We find a simple *closed* analytic expression for the expectation values of the Polyakov loop in all representations, valid in pure gauge theory as well as with dynamical quarks in an arbitrary representation. In Sec. 4 we show analogous results for aQCD. Finally, in Sec. 5 we summarize and conclude. Some technical details are deferred to the appendices. Throughout the paper, we use the natural units in which the Planck’s and Boltzmann’s constants as well as the speed of light are equal to one, and the timelike metric in the Minkowski space.

2. Model setup

In this section we set up the model that we later on use for numerical computations. In the gauge sector we employ a simple lattice-inspired model, which can in principle be used for any number of colors. The quark NJL Lagrangian derived afterwards is, as already stressed, applicable to all QCD-like theories with quarks in a real representation. This is natural: the Lagrangian is based almost exclusively on the flavor symmetry and is therefore valid for an arbitrary number of colors. The numerical values of the parameters in the model will be fixed in the following sections when we come to the discussion of concrete results.

2.1 Gauge sector

Our starting point for the pure gauge sector is an effective theory for the Polyakov loop

inspired by the lattice strong-coupling expansion. We closely follow the notation and line of argument of Ref. [20]. The action of the model is given by

$$\mathcal{S}_g[L] = -N_c^2 e^{-a/T} \sum_{\mathbf{x}, \mathbf{y}} \ell_{\mathbb{F}}(\mathbf{x}) \ell_{\mathbb{F}}^*(\mathbf{x} + \mathbf{y}), \quad (2.1)$$

where \mathbf{x} are the lattice sites and \mathbf{y} are the neighboring sites. (We use boldface to indicate spatial vectors.) The only adjustable parameter a is related to the string tension and can be extracted from numerical simulations of the full (pure) gauge theory. Furthermore, $\ell_{\mathbb{F}}(\mathbf{x}) \equiv \frac{1}{N_c} \text{Tr} L_{\mathbb{F}}(\mathbf{x})$ is the traced Polyakov loop in the fundamental representation; in the full gauge theory, the Polyakov loop in a given representation \mathcal{R} is defined as

$$L_{\mathcal{R}}(\mathbf{x}) \equiv \mathcal{P} \exp \left[i \int_0^{1/T} d\tau A_4^a(\mathbf{x}, \tau) T_{a\mathcal{R}} \right], \quad (2.2)$$

where $T_{a\mathcal{R}}$ are the gauge generators in this representation.

In the so-called Polyakov gauge where temporal gluons have constant values, this simplifies to

$$L_{\mathcal{R}}(\mathbf{x}) = \exp [i A_4^a(\mathbf{x}) T_{a\mathcal{R}} / T]. \quad (2.3)$$

Moreover, only the components of A_4^a corresponding to generators that form the Cartan subalgebra of the gauge group are nonzero. Let these components be $\theta_i T$. (There are $N_c - 1$ independent ones; the conventional factor T makes the variables θ_i dimensionless.) Each representation of the gauge group is characterized by a set of weights, $w_{i\alpha}$, that represent the eigenvalues of the generators of the Cartan subalgebra in this representation; the index α labels the different eigenvectors of the Cartan subalgebra. The traced Polyakov loop in representation \mathcal{R} then reads

$$\ell_{\mathcal{R}}(\mathbf{x}) = \frac{1}{\dim \mathcal{R}} \sum_{\alpha} e^{i\theta_i(\mathbf{x}) w_{i\alpha}}. \quad (2.4)$$

In the fundamental representation, the Polyakov loop (in the Polyakov gauge) is usually represented as $\text{diag}(e^{i\theta_1}, \dots, e^{i\theta_{N_c-1}}, e^{-i(\theta_1 + \dots + \theta_{N_c-1})})$. This corresponds to the choice of the N_c weights of the fundamental representation as $w_{i\alpha} = \delta_{i\alpha}$ for $\alpha = 1, \dots, N_c - 1$, and $w_{iN_c} = -1$ for all i . Equivalently, it can be written by defining $\theta_{N_c} = -(\theta_1 + \dots + \theta_{N_c-1})$ up to an integer multiple of 2π .

In the Weiss mean-field approximation, the nearest-neighbor interaction is linearized and the action (2.1) is replaced with the action $\mathcal{S}_{\text{mf}}(\alpha, \beta)$, depending on two mean fields α, β ,²

$$\mathcal{S}_{\text{mf}}(\alpha, \beta) = -N_c \sum_{\mathbf{x}} [\alpha \text{Re} \ell_{\mathbb{F}}(\mathbf{x}) + i\beta \text{Im} \ell_{\mathbb{F}}(\mathbf{x})]. \quad (2.5)$$

The dynamical variables of the model (2.1) are the (untraced) Polyakov loops $L(\mathbf{x})$ and its partition function is therefore obtained as $\mathcal{Z}_g \equiv \exp(-\Omega_g/T) = \int \prod_{\mathbf{x}} dL(\mathbf{x}) \exp(-\mathcal{S}_g[L])$, where dL is the group-invariant (Haar) measure on the $\text{SU}(N_c)$ gauge group. For the sake

²Here, we adhere to the notation introduced in Ref. [20]. Let us therefore just stress that the symbol β is not to be confused with the inverse temperature.

of future reference, let us add that in terms of the phases θ_i , the Haar measure can be written as

$$dL = \prod_{i=1}^{N_c-1} d\theta_i \prod_{i<j}^{N_c} |e^{i\theta_i} - e^{i\theta_j}|^2, \quad (2.6)$$

The integration over the variables θ_i is performed over the range $[0, 2\pi]$.

The thermodynamic potential can now be rewritten by subtracting and adding the mean-field action, resulting in the expression

$$\frac{\Omega_g}{T} = -\log \langle e^{-(\mathcal{S}_g - \mathcal{S}_{\text{mf}})} \rangle_{\text{mf}} - \log \int \prod_{\mathbf{x}} dL(\mathbf{x}) e^{-\mathcal{S}_{\text{mf}}}. \quad (2.7)$$

Here and in the following, $\langle \cdot \rangle_{\text{mf}}$ is the average with respect to the distribution defined by the mean-field action. For a given (not necessarily local) function $\mathcal{O}[L]$ of the Polyakov loop, it reads

$$\langle \mathcal{O} \rangle_{\text{mf}} = \frac{\int \prod_{\mathbf{x}} dL(\mathbf{x}) \mathcal{O}[L] e^{-\mathcal{S}_{\text{mf}}}}{\int \prod_{\mathbf{x}} dL(\mathbf{x}) e^{-\mathcal{S}_{\text{mf}}}}. \quad (2.8)$$

Note that when the function \mathcal{O} is local and does not depend explicitly on the coordinate, the product over lattice sites can be dropped.

Equation (2.7) is still exact; no approximation has been made so far. By the same token, the thermodynamic potential Ω_g is independent of the arbitrary variables α, β . In the Weiss mean-field approximation, one replaces $\langle e^{-(\mathcal{S}_g - \mathcal{S}_{\text{mf}})} \rangle_{\text{mf}}$ with $e^{-\langle \mathcal{S}_g - \mathcal{S}_{\text{mf}} \rangle_{\text{mf}}}$ [20]. The mean fields are then determined selfconsistently from the stationarity condition. In fact, as long as $\beta = 0$ so that the averaging is done with a real mean-field action, one can use Jensen's inequality³ to show that this approximation provides a strict upper bound for the exact free energy. Its optimum estimate is then obtained by minimizing with respect to α .

The final formula for the Weiss mean field gauge thermodynamic potential reads

$$\begin{aligned} \frac{\Omega_g^{\text{W}} a_s^3}{TV} = & -2(d-1)N_c^2 e^{-a/T} \langle \ell_{\text{F}} \rangle_{\text{mf}} \langle \ell_{\text{F}}^* \rangle_{\text{mf}} + \frac{N_c}{2} [(\alpha + \beta) \langle \ell_{\text{F}} \rangle_{\text{mf}} + (\alpha - \beta) \langle \ell_{\text{F}}^* \rangle_{\text{mf}}] - \\ & - \log \int dL e^{N_c(\alpha \text{Re } \ell_{\text{F}} + i\beta \text{Im } \ell_{\text{F}})}. \end{aligned} \quad (2.9)$$

Here a_s denotes the lattice spacing and the factor a_s^3/V is just the inverse of the number of lattice sites; d stands for the dimensionality of spacetime so that $2(d-1)$ is the number of nearest neighbors on a cubic lattice.

³Jensen's inequality (see e.g. Ref. [30]) states rather generally that for any real convex function f , $f(\langle x \rangle) \leq \langle f(x) \rangle$, where the averaging involves either a (weighted) arithmetic mean in the discrete version of the inequality, or an integral average over a given probability distribution in the continuous version.

2.2 Quark sector

The Lagrangian of the quark sector cannot be derived from the underlying gauge theory directly. However, it is strongly constrained by the requirement that it inherits all the symmetries of the QCD-like theory. As already stressed above, in theories with N_f massless quark flavors in a (pseudo)real representation of the gauge group, the usual chiral symmetry is promoted to $SU(2N_f)$. In order to see how this comes about, let us start from the Lagrangian of the gauge theory, including a common mass m_0 for all quark flavors,

$$\mathcal{L}_{\text{QCD-like}} = \bar{\psi} i \not{D} \psi - m_0 \bar{\psi} \psi, \quad (2.10)$$

where $\mathcal{D}_\mu \psi = (\partial_\mu - ig T_a A_\mu^a) \psi$ is the gauge-covariant derivative. Indices are suppressed so that this formula holds for quarks in any representation of the gauge group.

The fact that the quark representation is (pseudo)real means that there is a unitary matrix \mathcal{P} such that $\mathcal{P} \psi^\mathcal{C}$ has the same transformation properties under the gauge group as ψ . It is then advantageous to trade the Dirac spinor, consisting of the left- and right-handed components, for the purely left-handed Nambu spinor,

$$\Psi = \begin{pmatrix} \psi_L \\ \mathcal{P} \psi_R^\mathcal{C} \end{pmatrix}. \quad (2.11)$$

A crucial fact known from the theory of Lie algebras is that \mathcal{P} is either symmetric or antisymmetric according to whether the quark representation is real or pseudoreal [31]. Writing collectively $\mathcal{P}^T = \pm \mathcal{P}$, we can introduce the charge-conjugated Nambu spinor,

$$\Psi^\mathcal{C} = \mathcal{P} \begin{pmatrix} \psi_L^\mathcal{C} \\ (\mathcal{P} \psi_R^\mathcal{C})^\mathcal{C} \end{pmatrix} = \begin{pmatrix} \mathcal{P} \psi_L^\mathcal{C} \\ \pm \psi_R \end{pmatrix}. \quad (2.12)$$

The Dirac conjugate of both Ψ and $\Psi^\mathcal{C}$ is defined naturally by conjugating the individual components. The Lagrangian (2.10) then becomes, in the Nambu formalism,

$$\mathcal{L}_{\text{QCD-like}} = \bar{\Psi} i \not{D} \Psi - \left[\frac{1}{2} m_0 \bar{\Psi}^\mathcal{C} \begin{pmatrix} 0 & \mathbb{1} \\ \pm \mathbb{1} & 0 \end{pmatrix} \Psi + \text{H.c.} \right]. \quad (2.13)$$

First of all, we can see that in the chiral limit, the Lagrangian of a QCD-like theory indeed has an $SU(2N_f)$ symmetry. Note that baryon number is already incorporated in this simple group, for it is represented by the block matrix $\frac{1}{2} \text{diag}(\mathbb{1}, -\mathbb{1})$ in Nambu space. The change of the overall phase of the Nambu spinor corresponds to the axial $U(1)_A$ symmetry which is broken at the quantum level by instanton effects. Since the mass term has the same structure as the chiral condensate, we can also immediately infer that for type-I (type-II) theories the order parameter for flavor symmetry breaking transforms as a(n) (anti)symmetric rank-two tensor of $SU(2N_f)$. Therefore, the two classes of theories have different symmetry-breaking patterns and subsequently also different low-energy spectra. The symmetry-breaking patterns in the vacuum are $SU(2N_f) \rightarrow SO(2N_f)$ and $SU(2N_f) \rightarrow \text{Sp}(2N_f)$ for type I and type II, respectively [4].

The task to construct an NJL-type interaction compatible with the $SU(2N_f)$ symmetry is most easily accomplished using the Nambu notation (2.11). It is useful to stress right at the outset that as long as only color-singlet channels are considered, each of the Lagrangians to be constructed below applies to the whole class of QCD-like theories (type-I or type-II), regardless of the detailed structure of the gauge group or the quark representation. In fact, NJL Lagrangians for type-II theories with two quark flavors were already constructed in Ref. [11]. Here we follow the same line of argument with the necessary modifications for the type-I case.

One property that further distinguishes the type-I and type-II theories is the severity of the sign problem. While we remarked before that all QCD-like theories considered in this paper are free from the sign problem, one should be a bit careful with the type-II theories. There, the determinant of the Dirac operator is in general real, but needs not be positive. In order that there be no sign problem, one therefore has to consider an even number of flavors. On the other hand, type-I theories have no sign problem for any number of flavors [32]. As a warm-up exercise, we thus start with the simplest case of one flavor.

In the following, the Pauli matrices $\sigma_{0,1,2,3} = \{\mathbb{1}, \sigma_1, \sigma_2, \sigma_3\}$ are used to denote the block matrices in Nambu space, and $\tau_{0,1,2,3} = \{\mathbb{1}, \tau_1, \tau_2, \tau_3\}$ are used to denote the flavor generators for $N_f = 2$. The symmetric rank-two tensor representation of the flavor $SU(2) \simeq SO(3)$ group is real and three-dimensional. Using the basis of symmetric unimodular unitary matrices as $\vec{\Sigma} = \{\mathbb{1}, i\sigma_1, i\sigma_3\}$, we can immediately construct two four-fermion interaction terms,

$$\begin{aligned} \mathcal{L}_{1f,U(2)} &= G |\overline{\Psi}^{\mathcal{C}} \vec{\Sigma} \Psi|^2 = G [(\bar{\psi}\psi)^2 + (\bar{\psi}i\gamma_5\psi)^2 + |\overline{\psi}^{\mathcal{C}}\gamma_5\psi|^2 + |\overline{\psi}^{\mathcal{C}}\psi|^2], \\ \mathcal{L}_{1f,SU(2)} &= \frac{G}{2} [(\overline{\Psi}^{\mathcal{C}} \vec{\Sigma} \Psi)^2 + \text{H.c.}] = -G [(\bar{\psi}\psi)^2 - (\bar{\psi}i\gamma_5\psi)^2 + |\overline{\psi}^{\mathcal{C}}\gamma_5\psi|^2 - |\overline{\psi}^{\mathcal{C}}\psi|^2]. \end{aligned} \quad (2.14)$$

While the former preserves the axial $U(1)_A$, the latter breaks it explicitly. It is easy to verify that $\mathcal{L}_{1f,SU(2)}$ is the 't Hooft determinant term, i.e.

$$\mathcal{L}_{1f,SU(2)} = 2G(\det \overline{\Psi}_i^{\mathcal{C}} \Psi_j + \text{H.c.}). \quad (2.15)$$

For two flavors, the ten basis matrices of the symmetric rank-two tensor representation of the flavor $SU(4)$ are chosen as the symmetric Kronecker products of σ and τ , i.e.

$$\vec{\Sigma} = \{\sigma_{\text{sym}} \otimes \tau_{\text{sym}}, \sigma_{\text{antisym}} \otimes \tau_{\text{antisym}}\}. \quad (2.16)$$

Since the 10-dimensional representation of $SU(4)$ is complex, only one of the above two possibilities to construct an invariant interaction term remains,

$$\begin{aligned} \mathcal{L}_{2f,U(4)} &= G |\overline{\Psi}^{\mathcal{C}} \vec{\Sigma} \Psi|^2 \\ &= G \left[(\bar{\psi}\psi)^2 + (\bar{\psi}i\gamma_5\vec{\tau}\psi)^2 + (\bar{\psi}i\gamma_5\psi)^2 + (\bar{\psi}\vec{\tau}\psi)^2 + \sum_S |\overline{\psi}^{\mathcal{C}}\tau_S\psi|^2 + \sum_S |\overline{\psi}^{\mathcal{C}}\gamma_5\tau_S\psi|^2 \right], \end{aligned} \quad (2.17)$$

which preserves $U(1)_A$ automatically. (Here τ_S denotes the set of symmetric Pauli matrices, $\tau_S = \{\mathbb{1}, \tau_1, \tau_3\}$.) A $U(1)_A$ breaking interaction can again be introduced by the 't Hooft determinant term, but such a term will be an eight-fermion contact interaction which we do not consider in our model.

2.3 Mean-field approximation

We will employ the usual mean-field approximation, introducing the collective bosonic fields via the Hubbard–Stratonovich transformation and subsequently replacing them with their vacuum expectation values. To that end, however, one first needs to guess which condensates (order parameters) will appear in the phase diagram. The case of type-II theories with two quark flavors was worked out in Ref. [11]: as long as just the baryon chemical potential is considered, one only needs the chiral condensate, $\sigma = -2G\langle\bar{\psi}\psi\rangle$, and the scalar diquark condensate, $\Delta = 2iG\langle\psi^T C\gamma_5 \mathcal{P}\tau_2\psi\rangle$. Since the diquark wave function is antisymmetric in color as well as spin indices, it must, by means of the Pauli principle, also be antisymmetric with respect to flavor. The (spin-zero) diquark in type-II theories therefore mixes quarks of different flavors. Consequently, in the presence of an isospin chemical potential the diquark pairing feels stress and eventually diminishes via a first-order phase transition, with a narrow window of chemical potentials featuring inhomogeneous pairing [11, 33].

In type-I theories the scalar order parameters are symmetric in color and antisymmetric in spin indices, hence they must be symmetric in flavor. This is in accordance with the fact that for two flavors, there are altogether nine NG bosons of the $SU(4)/SO(4)$ coset, the isospin triplet of pions and the isospin triplet of (complex) diquarks. At zero isospin chemical potential, the isospin multiplets are strictly degenerate. In particular all uu , dd , and $ud + du$ diquarks can condense when the baryon chemical potential exceeds their common mass. However, for arbitrarily small isospin chemical potential, the diquarks formed from quarks of the same flavor will be favored. Such single-flavor condensates do not feel stress at nonzero chemical potential, and the phase diagram of type-I theories will therefore not contain inhomogeneous phases, as observed in Ref. [34].

With the above argument in mind, we restrict our attention to single-flavor condensates. The fact that the two-flavor four-fermion interaction (2.17) automatically preserves $U(1)_A$ means that the condensates differing just by opposite parity will be degenerate. However, we know from the Vafa–Witten theorem that in the vacuum parity is not spontaneously broken [35]. The degeneracy will be eventually lifted by instanton effects, manifested in the eight-quark ‘t Hooft interaction term. Within the present model, we will simply ignore the negative-parity channels.

As long as we only deal with one-flavor condensates, we can write down the contribution to the thermodynamic potential from a single quark flavor. This equals the thermodynamic potential of free fermionic quasiparticles. In presence of a pairing gap Δ , their dispersion relation reads $E_{\mathbf{k}}^e = \sqrt{(\xi_{\mathbf{k}}^e)^2 + \Delta^2}$, where $\xi_{\mathbf{k}}^e = \epsilon_{\mathbf{k}} + e\mu$, $e = \pm$, and $\epsilon_{\mathbf{k}} = \sqrt{\mathbf{k}^2 + M^2}$; $M = m_0 + \sigma$ is the constituent quark mass and μ the quark chemical potential. The gauge and quark sectors are coupled in the PNJL spirit [21]. In the Polyakov gauge the temporal component of the gauge field is constant. The individual quark color states in a given representation will then have, in the presence of the background gauge field, effective chemical potentials $iT \sum_i \theta_i w_{i\alpha}$. Since the quasiparticle spectrum discussed above is the same for all color states in the representation (this is because all condensates are color

singlets!), the thermodynamic potential of one quark flavor will simply be

$$\frac{\Omega_q}{VN_f} = \frac{\sigma^2 + \Delta^2}{4G} - \sum_e \int \frac{d^3\mathbf{k}}{(2\pi)^3} \times \left\{ E_{\mathbf{k}}^e \dim \mathcal{R} + 2T \log \left\langle \prod_{\alpha} \left[1 + 2 \cos(\theta_i w_{i\alpha}) e^{-E_{\mathbf{k}}^e/T} + e^{-2E_{\mathbf{k}}^e/T} \right]^{1/2} \right\rangle_{\text{mf}} \right\}. \quad (2.18)$$

The power of 1/2 in the second line compensates the doubling of the number of degrees of freedom in the Nambu formalism.

The group average must be performed once we couple the quarks to the Polyakov loop. Note that we do not average the full quark thermodynamic potential, but only the argument of the logarithm. This replacement was introduced in Eq. (13) of Ref. [20] as a convenient approximation to $\langle \Omega_q \rangle_{\text{mf}}$. However, in Appendix B we present a heuristic argument showing that the prescription (2.18) is actually superior to the full average $\langle \Omega_q \rangle_{\text{mf}}$. While with fundamental quarks considered in Ref. [20] the numerical difference between the two ways of evaluating the quark sector thermodynamic potential is negligible, we point out that with adjoint quarks, taking the average $\langle \Omega_q \rangle_{\text{mf}}$ would lead to unphysical artifacts which are not present in Eq. (2.18).

2.4 Parameter fixing in the quark sector

The NJL part of the model has three adjustable parameters: the coupling G , the current quark mass m_0 , and the ultraviolet cutoff that regulates divergent integrals. (Within this paper, we will use the three-momentum regularization scheme.) These need to be fixed by fitting to three selected observables. A conventional, and convenient, choice are the chiral condensate, pion mass, and decay constant in the vacuum. While the pion mass is more or less a free parameter that can be easily modified in lattice simulations by tuning the quark mass, the remaining two parameters depend on the single physical scale of the underlying theory, and cannot therefore be adjusted at will.

In three-color QCD with fundamental quarks, one can directly use experimental observables. In QC₂D, the input parameters were determined in Ref. [10] from their three-color counterparts by N_c -rescaling. Unfortunately, we are not aware of suitable lattice data that would allow us to fix the parameters directly in the case of aQCD and aQC₂D. We therefore use the following indirect argument. Suppose that we have a theory with both fundamental and adjoint quarks. Gauge invariance can then only be maintained when the coupling of quarks to gluons is the same in both representations. Since the effective meson-channel Lagrangians of the NJL type can be derived from a one-gluon-exchange-inspired interaction, this allows us to fix the ratio of the effective couplings in the fundamental and adjoint quarks sectors.

Concretely, assume the current-current interaction

$$\mathcal{L}_{\text{int}} = -g(\bar{\psi}\gamma^\mu T_{a\mathcal{R}}\psi)^2. \quad (2.19)$$

The coupling g can be directly related to the microscopic QCD coupling and the screening mass of the gluon in the one-gluon-exchange approximation. We therefore assume that it is

a [MeV]	$b^{1/3}$ [MeV]	Λ [MeV]	G [GeV $^{-2}$]	m_0 [MeV]
670.9	269.2	657	25.71	5.4

Table 1: Model parameters for two-color QCD with adjoint quarks.

the same for fundamental and adjoint quarks. Performing the Fierz transformation to the meson channel yields the effective NJL coupling $G_F = g(N_c^2 - 1)/(2N_c^2 N_f)$ for fundamental quarks [36]. For adjoint quarks we analogously obtain $G_A = gN_c/[(N_c^2 - 1)N_f]$. This results in the ratio

$$\frac{G_A}{G_F} = \frac{2N_c^3}{(N_c^2 - 1)^2}. \quad (2.20)$$

For the reader's convenience, the derivation of this relation is sketched in Appendix A. In the following sections, we will use it to infer the value of the coupling for adjoint quarks from that for the fundamental ones. We will not refer to the original current–current interaction anymore.

Eq. (2.20) would at first glance suggest that the coupling for adjoint quarks is weaker than for the fundamental ones (with the exception $N_c = 2$). One may then wonder why the chiral restoration temperature is much higher for adjoint quarks. The reason for this is that in the gap equation, the coupling is multiplied by the number of quark degrees of freedom coming from the quark loop. The effective coupling ratio for adjoint versus fundamental quarks therefore is $2N_c^2/(N_c^2 - 1)$ which is always larger than two.

3. Two colors

For two colors, the group integration is easily done and it is possible to find closed analytic expressions for all general formulas derived above. First, there is just one independent phase θ , associated with the only diagonal generator of the SU(2) gauge group. The $(2j + 1)$ -dimensional spin- j representation then has weights $-2j\theta, \dots, +2j\theta$, and one immediately obtains

$$\ell_j = \frac{1}{2j + 1} \frac{\sin(2j + 1)\theta}{\sin \theta}. \quad (3.1)$$

The Haar measure (2.6) reduces to $dL = \frac{1}{\pi} \sin^2 \theta d\theta$, normalized so that the group volume is unity.

Since all traced Polyakov loops of SU(2) are real, we need just one mean field α in Eq. (2.5). Using the definition of the modified Bessel function of integer order,

$$I_n(x) = \frac{1}{\pi} \int_0^\pi d\theta e^{x \cos \theta} \cos n\theta, \quad (3.2)$$

and the recurrence relation $I_{n-1}(x) - I_{n+1}(x) = \frac{2n}{x} I_n(x)$, one derives the expectation value of the Polyakov loops [37],

$$\langle \ell_j \rangle_{\text{mf}} = \frac{I_{2j+1}(2\alpha)}{I_1(2\alpha)}. \quad (3.3)$$

The gauge part of the thermodynamic potential (2.9) in turn becomes

$$\frac{\Omega_g^W}{V} = bT \left[-24e^{-a/T} \langle \ell_F \rangle_{\text{mf}}^2 + 2\alpha \langle \ell_F \rangle_{\text{mf}} - \log \frac{I_1(2\alpha)}{\alpha} \right], \quad (3.4)$$

where we denoted $b = a_s^{-3}$ to facilitate comparison with the “standard” PNJL model [10, 20]. The weights of the adjoint representation are $-2, 0, 2$ and the group average in the quark sector is also easily evaluated. The result is most conveniently written in terms of the expectation value of the adjoint Polyakov loop,

$$\frac{\Omega_q}{VN_f} = \frac{\sigma^2 + \Delta^2}{4G} - \sum_e \int \frac{d^3\mathbf{k}}{(2\pi)^3} \left[3E_{\mathbf{k}}^e + 2T \log(1 + e^{-E_{\mathbf{k}}^e/T}) + 2T \log(1 - e^{-E_{\mathbf{k}}^e/T} + e^{-2E_{\mathbf{k}}^e/T} + 3e^{-E_{\mathbf{k}}^e/T} \langle \ell_A \rangle_{\text{mf}}) \right]. \quad (3.5)$$

This is the formula that we use for the analysis of the phase diagram.

3.1 Phase diagram

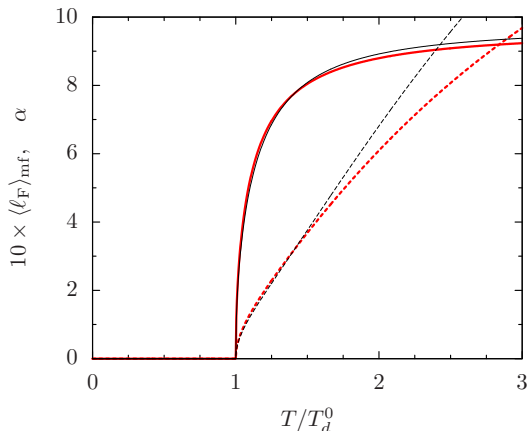


Figure 1: Comparison of the expectation values of the mean field α (dashed) and the fundamental Polyakov loop (solid) in the naive (thin black lines) and Weiss (thick red lines) mean-field approximations to the pure gauge theory.

obtained from the three-color pure gauge theory using their scaling properties in the limit of a large number of colors, so they do not quantitatively precisely agree with those one would obtain directly from the two-color lattice gauge theory. However, this does not matter since we do not fit the parameters in the quark sector to lattice data. Within this paper, we merely wish to demonstrate the general trends as the number of colors or the quark representation are varied.

Since we use a different potential for the Polyakov loop than in Ref. [10], the parameters a, b will actually take different values despite the same input for T_d^0 and σ_s . The deconfinement transition in the pure gauge theory is of second order with two colors, hence

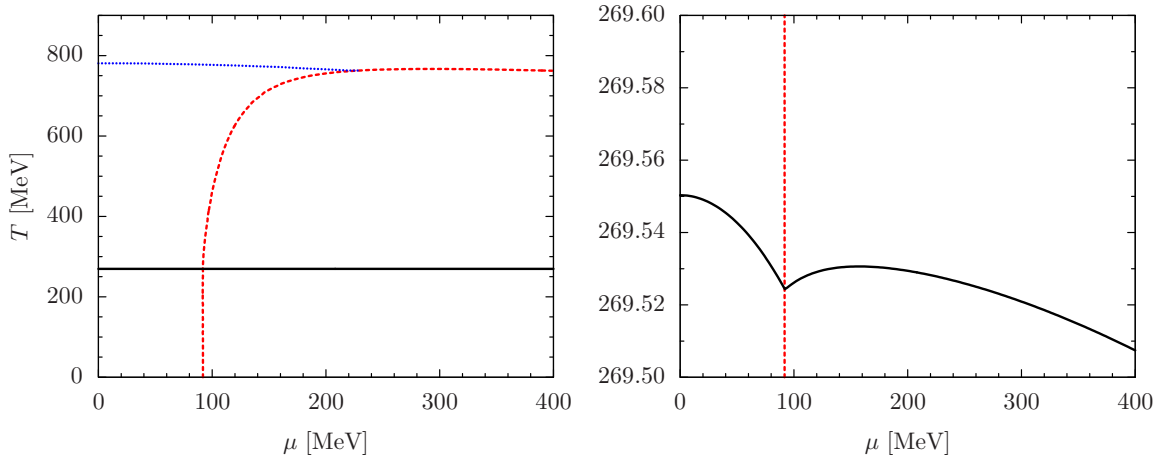


Figure 2: Phase diagram of two-color QCD with one flavor of adjoint quarks. Black solid line: deconfinement transition. Red dashed line: BEC transition. Blue dotted line: chiral crossover. The right panel zooms in the temperature scale so that the cusp in the deconfinement critical line is visible.

we can expand the thermodynamic potential (3.4) to second order in α ,

$$\frac{\Omega_g^W}{V} = bT\alpha^2 \left(\frac{1}{2} - 6e^{-a/T} \right) + \mathcal{O}(\alpha^4). \quad (3.6)$$

From here one concludes that $a = T_d^0 \log 12$. The lattice spacing a_s , hence the parameter b , is then determined from the strong-coupling relation $a = \sigma_s a_s$. The numerical values of all parameters are summarized in Tab. 1.

The Weiss mean-field approximation employed here differs from the mean-field approximation used in Ref. [10], which we will henceforth refer to as “naive” for reasons explained in Appendix B. In the latter, the gauge sector potential can be expressed solely in terms of the fundamental Polyakov loop and it reads,

$$\frac{\Omega_g^{\text{naive}}}{V} = -bT [24e^{-a/T} \ell_F^2 + \log(1 - \ell_F^2)], \quad (3.7)$$

cf. Eq. (3.4). It is therefore mandatory to compare the results obtained with the two approaches. We do so within the pure gauge theory. The expectation values of the fundamental Polyakov loop and the mean field α are shown in Fig. 1.⁴ It is obvious that the results for the Polyakov loop are not sensitive to the particular implementation of the gauge sector as long as the parameters are adjusted to reproduce the same physical observables.

Figure 2 shows the phase diagram of aQC₂D with one quark flavor in the plane of temperature and quark chemical potential. The deconfinement transition associated with the breaking of center Z_2 is denoted by the black solid line, while the BEC transition at which the baryon number $U(1)_B$ is broken is indicated by the red dashed line. In addition to

⁴Note that there is no α in the naive mean-field approximation. The values plotted in Fig. 1 were obtained by inverting the relation (3.3).

these two sharp phase transitions, there is a smooth crossover associated with the melting of the chiral condensate. Its position, shown in the left panel of Fig. 2 by the blue dotted line, is defined here by the maximum temperature gradient of σ . In the chiral limit, this also becomes a sharp second-order phase transition. As expected, it does appear at a temperature much higher than that of the deconfining transition ($T_d = 270$ MeV, while $T_\chi = 780$ MeV so that $T_\chi/T_d = 2.89$). However, the precise value of this temperature as determined by our model is strongly affected by the cutoff, as is discussed in more detail in Sec. 4.1.

The temperature of the deconfining transition depends on the chemical potential extremely weakly, even less than in QC₂D [10]. The reason apparently is that the adjoint quarks are neutral with respect to the center symmetry. The behavior of the transition lines in the vicinity of their “intersection” will be analyzed in detail in the following subsection. Finally, the BEC transition at zero temperature occurs at $\mu = 92$ MeV, which is in a good agreement with the fact that the mass of the pion/diquark multiplet in the vacuum is $m_\pi = 184$ MeV within our parameter set.

As an illustration of the solution of the gap equations, we plot in Fig. 3 the condensates at $\mu = 100$ MeV as a function of temperature. One can clearly see the effect of the suppression of thermal quark fluctuations in the confined phase: the condensates are nearly constant for $T < T_d$.

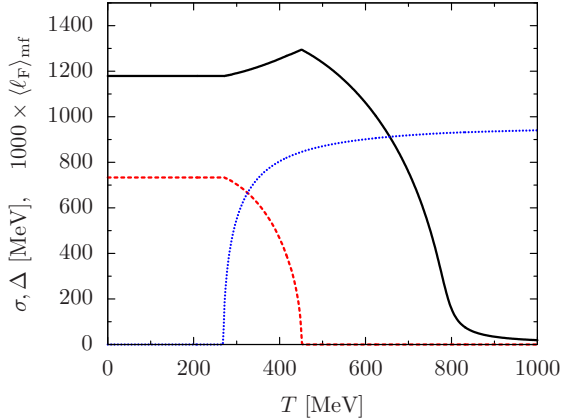


Figure 3: Condensates in aQC₂D at $\mu = 100$ MeV as a function of temperature. The chiral condensate σ (black solid line), diquark condensate Δ (red dashed line), and the fundamental Polyakov loop (blue dotted line) are shown.

3.2 Tetracritical point

At the point where the two second-order transition lines cross, the system exhibits tetracritical behavior [14]. Here we will analyze the details of the phase transitions in the vicinity of the tetracritical point using the GL theory. The thermodynamic potential depends on three mean fields, α, σ, Δ . Only two of them, α and Δ , comprise order parameters for spontaneous symmetry breaking of an exact symmetry (unless we consider the chiral limit). In order to construct the GL free energy, one therefore needs to eliminate σ in favor of α, Δ by means of its gap equation. Around the tetracritical point, we can then perform a double Taylor expansion of the total thermodynamic potential, $\Omega = \Omega_g^W + \Omega_q$. Thanks to the Z_2 and $U(1)_B$ symmetries, it depends just on the squares of the mean fields,

$$\frac{\Omega(\alpha^2, \Delta^2)}{V} = b_\alpha \alpha^2 + b_\Delta \Delta^2 + \frac{1}{2} [\lambda_{\alpha\alpha} (\alpha^2)^2 + 2\lambda_{\alpha\Delta} \alpha^2 \Delta^2 + \lambda_{\Delta\Delta} (\Delta^2)^2]. \quad (3.8)$$

The effective quartic couplings are determined by the second *total* derivatives of the ther-

modynamic potential,

$$\lambda_{\alpha\alpha} = \frac{1}{V} \frac{d^2\Omega}{d(\alpha^2)^2}, \quad \lambda_{\alpha\Delta} = \frac{1}{V} \frac{d^2\Omega}{d\alpha^2 d\Delta^2}, \quad \lambda_{\Delta\Delta} = \frac{1}{V} \frac{d^2\Omega}{d(\Delta^2)^2}, \quad (3.9)$$

evaluated at $\alpha = \Delta = 0$. These total derivatives are in turn given in terms of the partial derivatives of the thermodynamic potential as a function of all three mean fields,

$$\frac{d^2\Omega}{d\chi_i d\chi_j} = \frac{\partial^2\Omega}{\partial\chi_i \partial\chi_j} - \frac{\partial^2\Omega}{\partial\chi_i \partial\sigma} \left(\frac{\partial^2\Omega}{\partial\sigma^2} \right)^{-1} \frac{\partial^2\Omega}{\partial\sigma \partial\chi_j}, \quad (3.10)$$

where χ_i stands for α^2, Δ^2 . In order to evaluate the GL quartic couplings, we need to know six second partial derivatives of the thermodynamic potential,

$$\begin{aligned} \frac{\partial_{\alpha^2\alpha^2}\Omega}{V} &= \frac{1}{4}bT \left(16e^{-a/T} - 1 \right) + N_f T \sum_e \int \frac{d^3\mathbf{k}}{(2\pi)^3} \frac{\cosh(\xi_{\mathbf{k}}^e/T)}{[2\cosh(\xi_{\mathbf{k}}^e/T) - 1]^2}, \\ \frac{\partial_{\alpha^2\Delta^2}\Omega}{V} &= N_f \sum_e \int \frac{d^3\mathbf{k}}{(2\pi)^3} \frac{\sinh(\xi_{\mathbf{k}}^e/T)}{\xi_{\mathbf{k}}^e} \frac{1}{[2\cosh(\xi_{\mathbf{k}}^e/T) - 1]^2}, \\ \frac{\partial_{\Delta^2\Delta^2}\Omega}{V} &= \frac{3}{4}N_f \sum_e \int \frac{d^3\mathbf{k}}{(2\pi)^3} \frac{1}{(\xi_{\mathbf{k}}^e)^3} \left[\tanh \frac{3\xi_{\mathbf{k}}^e}{2T} - \frac{3\xi_{\mathbf{k}}^e}{2T \cosh^2(3\xi_{\mathbf{k}}^e/2T)} \right], \\ \frac{\partial_{\sigma\alpha^2}\Omega}{V} &= 2MN_f \sum_e \int \frac{d^3\mathbf{k}}{(2\pi)^3} \frac{1}{\epsilon_{\mathbf{k}}} \frac{\sinh(\xi_{\mathbf{k}}^e/T)}{[2\cosh(\xi_{\mathbf{k}}^e/T) - 1]^2}, \\ \frac{\partial_{\sigma\Delta^2}\Omega}{V} &= \frac{3}{2}MN_f \sum_e \int \frac{d^3\mathbf{k}}{(2\pi)^3} \frac{1}{\epsilon_{\mathbf{k}}(\xi_{\mathbf{k}}^e)^2} \left[\tanh \frac{3\xi_{\mathbf{k}}^e}{2T} - \frac{3\xi_{\mathbf{k}}^e}{2T \cosh^2(3\xi_{\mathbf{k}}^e/2T)} \right], \\ \frac{\partial_{\sigma\sigma}\Omega}{V} &= \frac{N_f m_0}{2G M} + 3M^2 N_f \sum_e \int \frac{d^3\mathbf{k}}{(2\pi)^3} \frac{1}{\epsilon_{\mathbf{k}}^3} \left[\tanh \frac{3\xi_{\mathbf{k}}^e}{2T} - \frac{3\epsilon_{\mathbf{k}}}{2T \cosh^2(3\xi_{\mathbf{k}}^e/2T)} \right]. \end{aligned} \quad (3.11)$$

In order to see how the two condensates affect each other close to the tetracritical point, consider the general GL functional with two order parameters $\phi_{1,2}$ and assume it is constrained to have the form

$$\frac{\Omega(\phi_1, \phi_2)}{V} = b_1\phi_1^2 + b_2\phi_2^2 + \frac{1}{2}(\lambda_{11}\phi_1^4 + 2\lambda_{12}\phi_1^2\phi_2^2 + \lambda_{22}\phi_2^4). \quad (3.12)$$

[In our case, all other terms are prohibited by the Z_2 and $U(1)_B$ symmetries.] The phase diagram of such a model is depicted in Fig. 4. If only one condensate were present, the position of the phase transition would be determined by the point where the respective b coefficient changes sign. However, when both condensates are present, the transition lines shift. This is most easily seen from the expression for the nontrivial solution to the gap equations with both order parameters being nonzero,

$$\phi_1^2 = \frac{-\lambda_{22}b_1 + \lambda_{12}b_2}{\lambda_{11}\lambda_{22} - \lambda_{12}^2}, \quad \phi_2^2 = \frac{\lambda_{12}b_1 - \lambda_{11}b_2}{\lambda_{11}\lambda_{22} - \lambda_{12}^2}. \quad (3.13)$$

We can therefore see that the size of the region with both condensates depends on the sign and magnitude of the offdiagonal coupling λ_{12} .

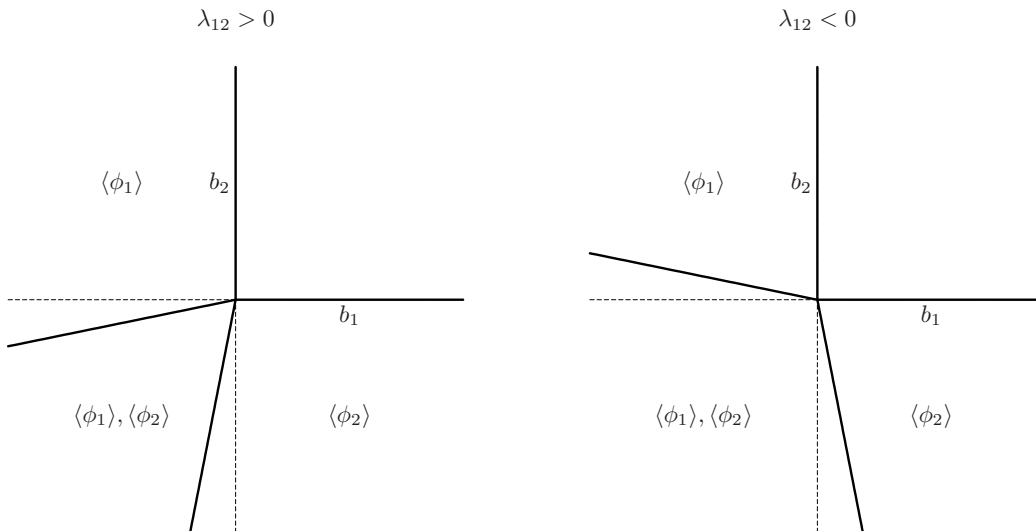


Figure 4: Schematic phase diagram of the Ginzburg–Landau theory with two order parameters. Thick lines denote second-order phase transitions. The labels indicate which order parameters take nonzero values in a given phase.

The description of the phase transitions based on the GL theory is universal and model independent as long as it captures the correct degrees of freedom and symmetries. A nontrivial task in general is to find the mapping of the (b_1, b_2) plane displayed in Fig. 4 to the physical observables, in our case the temperature and chemical potential. Even though this is in principle possible with our PNJL model, in the present work we performed just a basic compatibility check. Evaluating the GL coefficients for our parameter set using Eq. (3.11), one finds that $\lambda_{\alpha\alpha} \approx 2.3 \times 10^{-3} \Lambda^4$, $\lambda_{\alpha\Delta} \approx 5.7 \times 10^{-7} \Lambda^2$, and $\lambda_{\Delta\Delta} \approx 9.7 \times 10^{-6}$. The offdiagonal coupling is positive which means that the two condensates “repel” each other as in the left panel of Fig. 4. However, since the GL couplings are numerically very small, the angles between the critical lines hardly change at the tetracritical point. The slight deflection of the BEC transition line is visible in the left panel of Fig. 2. That the same happens to the deconfinement line is made manifest by the detail of the critical line shown in the right panel of Fig. 2.

3.3 Casimir scaling

The Casimir scaling hypothesis [37, 38] states that the color-singlet potential between a static quark and antiquark at intermediate distance is proportional to the quadratic Casimir invariant, $C_2(\mathcal{R})$, of the representation \mathcal{R} of the quarks. This statement is exact at two-loop order in perturbation theory [39] and receives corrections only at three-loop order [40]. At the same time, there is compelling evidence from lattice simulations that it holds to a high accuracy even in the nonperturbative regime [19, 41, 42, 43]. It may thus provide a handle to understand the nonperturbative behavior of QCD-like theories, and as such should be a necessary ingredient in any model attempting to mimic QCD (thermo)dynamics [44].

In the PNJL model, one cannot directly access the confining potential feature of QCD. However, the scaling of the static potential implies an analogous property of the expectation

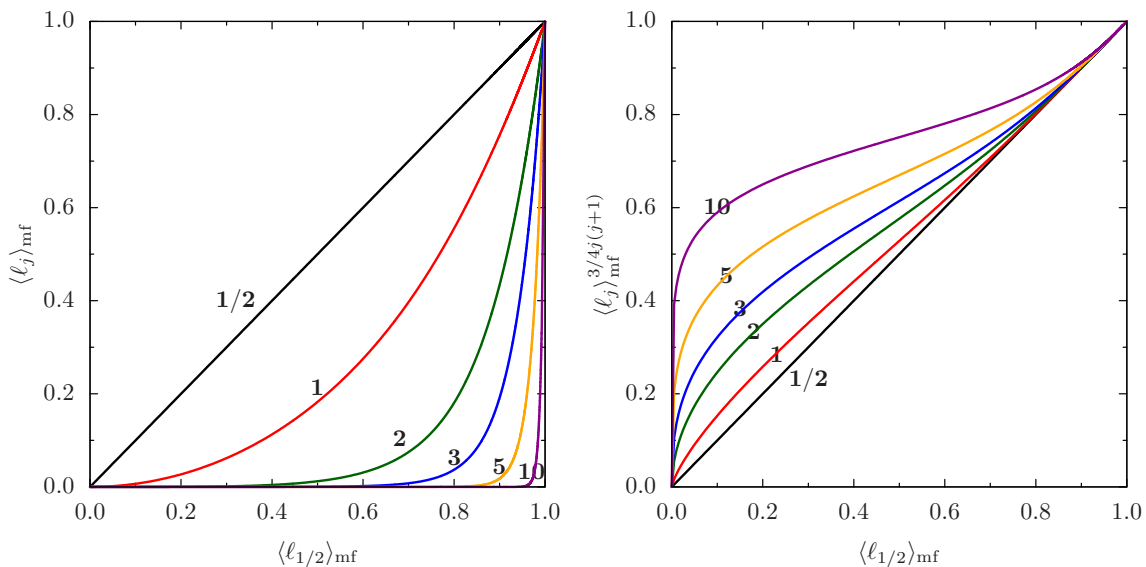


Figure 5: Expectation values of the Polyakov loops in various representations as a function of the fundamental Polyakov loop in the case of two colors. Boldface numbers indicate the “spin” j of the representation. Left panel: unscaled Polyakov loops. Right panel: Casimir-scaled Polyakov loops. For convenience, we take the $C_2(\mathcal{F})/C_2(\mathcal{R})$ power of the expectation values of the Polyakov loops so that the fundamental loop is left intact.

values of the Polyakov loops [19, 45]: the quantity $\langle \ell_{\mathcal{R}} \rangle_{\text{mf}}^{1/C_2(\mathcal{R})}$ should be independent of the representation \mathcal{R} . Since we have the analytic formula (3.3) for the expectation values of all Polyakov loops in two-color QCD, where one has simply $C_2(j) = j(j+1)$, we can easily check to what extent Casimir scaling is satisfied by our model.

Note that the expectation values of all Polyakov loops are expressed in terms of the mean field α , which can in turn be traded for the fundamental loop. In Fig. 5 we therefore plot the expectation values of the Polyakov loops in selected representations against that in the fundamental representation [19, 46]. Comparing the left and right panels that display the unscaled and scaled Polyakov loops, we can see that the Casimir scaling is very well reproduced as the value of the fundamental loop approaches one, which corresponds to high temperatures. It becomes worse at low temperatures, where the nearest-neighbor interaction model (2.1) is too oversimplified. Lattice data that hint at almost exact scaling even at low temperatures can be reproduced more satisfactorily once we add more terms including higher representation Polyakov loops in Eq. (2.1) [19].

Within our model, we can check even analytically how well Casimir scaling is satisfied at high temperatures, and hence, at high values of α . Carrying out the Taylor expansion of Eq. (3.3) around $\alpha = +\infty$, one finds

$$\langle \ell_j \rangle_{\text{mf}}^{1/j(j+1)} = 1 - \frac{1}{\alpha} + \frac{1}{4\alpha^2} + \frac{j^2 + j - \frac{1}{8}}{12\alpha^3} + \mathcal{O}\left(\frac{1}{\alpha^4}\right). \quad (3.14)$$

We can see that Casimir scaling is only violated at the fourth order of the expansion.

One important observation regarding our results in Fig. 5 is that they are based just on the group average (2.8) and do not make any reference to the quark sector of the model. Therefore, they apply equally well to two-color QCD with quarks in *any* representation as well as to the pure gauge theory. In particular, the same curves hold even for nonzero chemical potential, which provides us with a unique opportunity to study Casimir scaling at nonzero baryon density. The quark sector will just affect the dependence of the mean field α on the temperature and chemical potential, and therefore the speed at which the curves are traversed as T and μ vary.

4. Three colors

For three colors, the group integration is performed with the measure

$$dL = \frac{d\theta_1 d\theta_2}{6\pi^2} [\sin(\theta_1 - \theta_2) - \sin(2\theta_1 + \theta_2) + \sin(\theta_1 + 2\theta_2)]^2. \quad (4.1)$$

Three-color QCD with fundamental quarks has a charge conjugation invariance, which is implemented in the PNJL model by a simultaneous change $\theta_i \rightarrow -\theta_i$, $\mu \rightarrow -\mu$. Therefore, at any fixed nonzero chemical potential this charge conjugation invariance is explicitly broken. As a result, the expectation values $\langle \ell_F \rangle$ and $\langle \ell_F^* \rangle$ split. At the same time, the mean-field β becomes nonzero [20].

On the other hand, the situation in aQCD is different. Thanks to the reality of the gauge group representation, the nonzero weights appear in pairs with opposite sign. Consequently, the theory is invariant under *separate* charge conjugation in the quark and gluon sectors. The charge conjugation invariance in the gauge sector guarantees that the Polyakov loop in a given (e.g. fundamental) representation and its complex conjugate always have the same expectation value. We may therefore dispense with the mean field β , which greatly simplifies the group integration. In the gauge sector one can still obtain an analytic expression for the thermodynamic potential, albeit in the form of an infinite series [18]. One defines a function

$$F(\alpha) = \sum_{m=-\infty}^{+\infty} \det I_{m+i-j}(\alpha), \quad (4.2)$$

where the determinant is taken with respect to the indices i, j . One then finds the following expression for the thermodynamic potential,

$$\frac{\Omega_g^W a_s^3}{TV} = -6e^{-a/T} \left[\frac{F'(\alpha)}{F(\alpha)} \right]^2 + \alpha \frac{F'(\alpha)}{F(\alpha)} - \log F(\alpha), \quad (4.3)$$

and the expectation value of the fundamental Polyakov loop,

$$\langle \ell_F \rangle_{\text{mf}} = \frac{1}{N_c} \frac{F'(\alpha)}{F(\alpha)}. \quad (4.4)$$

The derivation of this formula is deferred to Appendix C where it will be generalized and used to write analytic expressions for the expectation values of all Polyakov loops.

a [MeV]	$b^{1/3}$ [MeV]	Λ [MeV]	G [GeV $^{-2}$]	m_0 [MeV]
542.1	333.2	651	8.51	5.5

Table 2: Model parameters for three-color QCD with adjoint quarks.

The eigenvalues of the Polyakov loop in the adjoint representation are 1 [($N_c - 1$)-times degenerate] and $e^{i(\theta_i - \theta_j)}$ for all pairs $i \neq j$. The logarithmic term in Eq. (2.18) becomes

$$2 \log \left\langle (1+x)^{N_c-1} \prod_{i < j}^{N_c} [1 + 2x \cos(\theta_i - \theta_j) + x^2] \right\rangle_{\text{mf}}, \quad (4.5)$$

where we abbreviated $x = e^{-E_{\mathbf{k}}^e/T}$. Specifically for three colors this is equal to

$$2 \log \left\{ (1+x)^2 [1 + 2x\omega_1 + x^2(3 + 4\omega_2) + 4x^3(\omega_1 + 2\omega_3) + x^4(3 + 4\omega_2) + 2x^5\omega_1 + x^6] \right\}. \quad (4.6)$$

Group integration reduces to evaluation of three averages,

$$\begin{aligned} \omega_1 &= \langle \cos(\theta_1 - \theta_2) + \cos(\theta_2 - \theta_3) + \cos(\theta_3 - \theta_1) \rangle_{\text{mf}}, \\ \omega_2 &= \langle \cos(\theta_1 - \theta_2) \cos(\theta_3 - \theta_1) + \cos(\theta_2 - \theta_3) \cos(\theta_1 - \theta_2) + \cos(\theta_3 - \theta_1) \cos(\theta_2 - \theta_3) \rangle_{\text{mf}}, \\ \omega_3 &= \langle \cos(\theta_1 - \theta_2) \cos(\theta_2 - \theta_3) \cos(\theta_3 - \theta_1) \rangle_{\text{mf}}. \end{aligned} \quad (4.7)$$

These can be performed independently of the value of x , so the evaluation of the quark thermodynamic potential factorizes into a one-dimensional momentum integral and a two-dimensional group integration. The latter can be performed either numerically or even analytically in a fashion similar to Eq. (4.2), as sketched in Appendix C.

4.1 Phase diagram

Again, we fix the parameters for the subsequent numerical computations first. The parameter a is determined by the deconfinement temperature T_d^0 in the pure gauge theory. With the thermodynamic potential (4.3), this corresponds to $e^{-a/T_d^0} = 0.13427$. Demanding $T_d^0 = 270$ MeV, this yields $a = 542.1$ MeV. The parameter b is in turn obtained from the physical string tension $\sigma_s = (425 \text{ MeV})^2$, as in the two-color case. In the NJL sector, we use the parameters of the two-flavor model with fundamental quarks, $\Lambda = 651$ MeV, $G = 5.04 \text{ GeV}^{-2}$, $m_0 = 5.5$ MeV, fitted to reproduce the pion mass and decay constant and the chiral condensate in the vacuum (see, for instance, Ref. [23]). The coupling is rescaled by the factor $27/32$ in accord with Eq. (2.20), and an additional factor of two to account for the fact that we deal just with one flavor here. The values of all parameters used in our calculations are summarized in Tab. 2.

As a basic cross-check we again evaluated first the deconfinement and chiral restoration temperatures (in the chiral limit) at zero chemical potential. The values $T_d = 270$ MeV and $T_\chi = 663$ MeV yield the ratio $T_\chi/T_d = 2.46$. This is quite far from the value ≈ 8 measured on the lattice [27, 28]. (Note that in Ref. [12] the lattice value of this ratio was

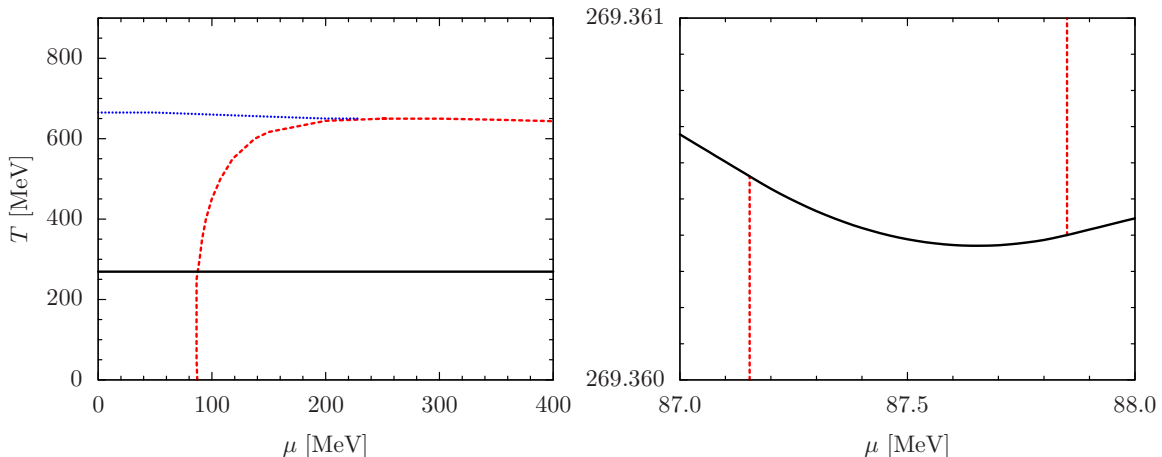


Figure 6: Phase diagram of three-color QCD with one flavor of adjoint quarks. Black solid line: deconfinement transition. Red dashed line: BEC transition. Blue dotted line: chiral crossover. The right panel zooms in the chemical potential and temperature scales so that the two tricritical points are discernible.

achieved by tuning the parameters of the model.) However, one should keep in mind that we made just a rough estimate of the NJL coupling G and cutoff Λ , on which the chiral restoration temperature depends very sensitively. In principle, one could use the lattice value for the ratio T_χ/T_d as an input in the model. Nevertheless, one cannot really hope to describe the chiral restoration in a quantitatively satisfactory manner within our model. The first reason is that at such high temperatures, the calculation of the thermodynamic potential is plagued by cutoff artifacts. (We regulate the whole quark contribution to the thermodynamic potential, including its finite thermal part.) The second reason is that the PNJL model ceases to be physically appropriate at temperatures about two to three times T_d [25], since it does not capture the correct gauge degrees of freedom, that is, the deconfined transversely polarized gluons. We are therefore just content with demonstrating that QCD with adjoint quarks indeed features a large splitting of the deconfinement and chiral restoration temperatures.

The phase diagram of aQCD determined within our PNJL model is shown in Fig. 6. While on the large scale it looks the same as the phase diagram of aQC₂D in Fig. 2, there is a marked difference in the topology as one zooms in the neighborhood of the “intersection” of the deconfinement and BEC transition lines. Since the deconfinement transition is now first order, the BEC critical line is broken, meeting the deconfinement line at two tricritical points. Thus, there is a narrow range of chemical potentials in which, as the temperature is increased, the diquark condensate rather unusually disappears in a first-order phase transition.

4.2 Casimir scaling

Any irreducible representation of SU(3) can be uniquely characterized by a pair of positive integers (p, q) that determine the highest weight of the representation in the basis of the

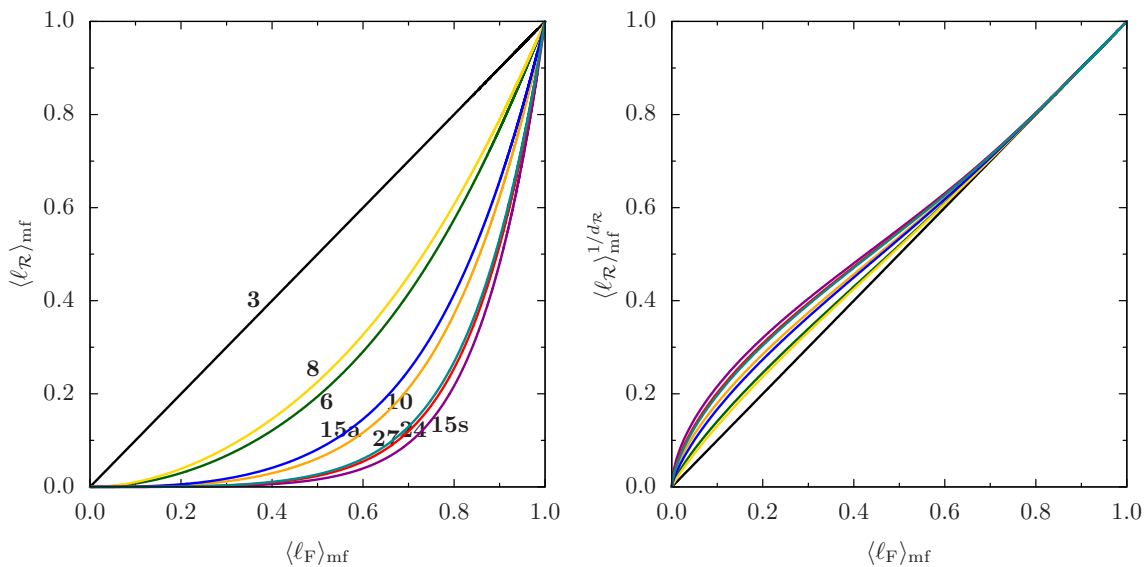


Figure 7: Expectation values of the Polyakov loops in various representations as a function of the fundamental Polyakov loop in the case of three colors. Boldface numbers indicate the dimension (and possibly the symmetry) of the representation. Left panel: unscaled Polyakov loops. Right panel: Casimir-scaled Polyakov loops. For convenience, we take the $C_2(\text{F})/C_2(\mathcal{R}) \equiv 1/d_{\mathcal{R}}$ power of the expectation values of the Polyakov loops so that the fundamental loop is left intact. For the sake of clarity, the labels are not shown in the right panel. The color assignment of the lines is the same as in the left panel.

fundamental weights. The triplet representation thus corresponds to $(1, 0)$ and its complex conjugate to $(0, 1)$. The dimension of a general irreducible representation is $\dim(p, q) = \frac{1}{2}(p+1)(q+1)(p+q+2)$ and the value of the quadratic Casimir invariant (up to a common prefactor) is $C_2(p, q) = \frac{1}{3}(p^2 + pq + q^2) + p + q$ [47]. Following Refs. [20, 42], we have calculated the expectation values of the Polyakov loops in the lowest few representations, satisfying $p + q \leq 4$. The results are shown in Fig. 7.

As before, these results are largely independent of the quark content of the theory. The only assumption made is that the mean field β is zero so that there is a one-to-one correspondence between the mean field α and the expectation value of the fundamental Polyakov loop. Thus, the plots in Fig. 7 apply to three-color QCD modeled by the action (2.1) with quarks in *any* representation at zero chemical potential. Once the quark representation is (pseudo)real, the same results are valid even at nonzero chemical potential. As compared to the two-color case shown in Fig. 5, the scaling violation seems to be significantly smaller for three colors. However, this observation is somewhat misleading since even the unscaled Polyakov loops show smaller depletion compared to the fundamental loop in the three-color case.

5. Conclusions

In the present paper, we worked out a description of the thermodynamics of QCD-like

theories at nonzero temperature and baryon chemical potential based on the PNJL model. To mimic the gauge sector we used a lattice spin model with nearest-neighbor interactions whose parameters are fixed with the help of the strong-coupling expansion of the full lattice gauge theory. The quark sector was modeled using the standard NJL model.

We derived a simple mean-field expression for the thermodynamic potential, which is applicable to QCD-like theories with any number of colors and with quarks in any representation, as long as this representation is (pseudo)real. In a sequel to Ref. [11], we constructed the NJL Lagrangians for the two classes of QCD-like theories, denoted as type I and type II.

We showed at hand of the example of QCD with adjoint quarks that the Weiss mean-field approximation to the lattice spin model used here is superior to the naive mean-field approximation, commonly employed in literature, which leads to a thermodynamic instability. The Weiss mean-field approximation also allowed us to derive the expectation value of the Polyakov loop in an arbitrary representation. The results are given in an implicit form applicable at all temperatures and chemical potentials, which enables us to study Casimir scaling in hot and/or dense matter.

As a concrete example, we studied the phase diagram of QCD with adjoint quarks of two and three colors. We confirmed that in adjoint QCD the critical temperature for chiral restoration is much higher than that of deconfinement, both being well-defined phase transitions associated with spontaneous breaking/restoration of an exact symmetry (the former in the chiral limit). We checked the model-independent prediction that the phase diagram of aQC₂D features a tetracritical point. On the contrary, in the phase diagram of aQCD the second-order BEC transition line is interrupted and meets the first-order deconfinement line at two tricritical points.

It is worth emphasizing that while fine numerical details of our phase diagrams depend on our guess for the model parameters as well as on the particular way quarks are implemented, their qualitative features are largely based on symmetry and thus model-independent. Moreover, our results for Casimir scaling do not depend on the quark sector, in particular on the choice of the NJL parameters. They can therefore be understood as a direct test of the lattice spin model with nearest-neighbor interactions. Once a model for the quark sector is introduced, they give a prediction for Casimir scaling of Polyakov-loop expectation values in the whole phase diagram.

In view of the recent lattice data [48, 49], the study of QCD-like theories offers a unique opportunity to gain more insight in the nature of strongly interacting dense matter. Even though all physical predictions eventually have to be made within the full gauge theory, we hope to have demonstrated that the PNJL model provides a versatile tool suitable for quick calculations and qualitative checks of the robust properties of the theory.

Acknowledgments

The authors are indebted to H. Abuki and K. Fukushima for numerous helpful discussions. Part of the work was carried out during the stay of T.B. at the Norwegian University of Science and Technology, Trondheim. T.B. would also like to gratefully acknowledge the warm

hospitality of the Department of Energy’s Institute for Nuclear Theory at the University of Washington, where the manuscript was completed. The research of T.Z. was supported by the German Academic Exchange Service (DAAD) and by the Helmholtz Graduate School for Hadron and Ion Research. The research of T.B. and D.H.R. was supported in part by the ExtreMe Matter Institute EMMI in the framework of the Helmholtz Alliance Program of the Helmholtz Association (HA216/EMMI).

A. Fierz transformation of the current–current interaction

Consider a fermionic field ψ transforming in a representation \mathcal{R} of the symmetry group. In NJL-like models, one deals with contact four-fermion interactions of the type $\sum_a (\bar{\psi}\Gamma_a^{\mathcal{A}}\psi)^2$, where $\Gamma_a^{\mathcal{A}}$ is a set of matrices that project out a particular irreducible component \mathcal{A} of the product representation $\overline{\mathcal{R}} \otimes \mathcal{R}$. The Fierz rearrangement of the four-fermion interaction is equivalent to the group-theoretical identity

$$\sum_a (\Gamma_a^{\mathcal{A}})_{ij} (\Gamma_a^{\mathcal{A}})_{kl} = \sum_{\mathcal{B}} C_{\mathcal{A}\mathcal{B}} \sum_b (\Gamma_b^{\mathcal{B}})_{il} (\Gamma_b^{\mathcal{B}})_{kj}, \quad (\text{A.1})$$

where the coefficients $C_{\mathcal{A}\mathcal{B}}$ depend only on the representations \mathcal{A}, \mathcal{B} . In order to fix the effective coupling in the meson channel, we need not evaluate the Fierz coefficients for all \mathcal{B} . All we need to know is the coefficient for the one-dimensional representation $\mathcal{B} = \mathcal{I}$, which is always contained in the product $\overline{\mathcal{R}} \otimes \mathcal{R}$.

Setting $\Gamma^{\mathcal{I}} = \mathbb{1}$, the coefficient $C_{\mathcal{A}\mathcal{I}}$ is projected out by multiplying Eq. (A.1) by $\delta_{li}\delta_{jk}$, which yields

$$C_{\mathcal{A}\mathcal{I}} = \frac{\sum_a \text{Tr}(\Gamma_a^{\mathcal{A}}\Gamma_a^{\mathcal{A}})}{(\dim \mathcal{R})^2}. \quad (\text{A.2})$$

In particular for $\mathcal{A} = \mathcal{I}$ this leads to $C_{\mathcal{I}\mathcal{I}} = 1/\dim \mathcal{R}$. This explains the $1/N_f$ factor in the effective NJL couplings derived from the current–current interaction (2.19): both the original interaction as well as the term $(\bar{\psi}\psi)^2$ whose coefficient we calculate are in the flavor-singlet channel. Likewise, the Fierz transformation from the Lorentz-vector channel to the Lorentz-scalar channel has the Fierz coefficient one.

The color structure of the current–current interaction (2.19) is such that \mathcal{A} corresponds to the adjoint representation, that is, $\Gamma_a^{\mathcal{A}} = T_{a\mathcal{R}}$ are the generators of the color group in the representation \mathcal{R} of the quark fields. The Fierz coefficient (A.2) then reduces to $C_{\mathcal{A}\mathcal{I}} = C_2(\mathcal{R})/\dim \mathcal{R}$. Specifically for the $SU(N)$ group, once the generators in the fundamental representation are normalized as $\text{Tr}(T_{a\mathcal{F}}T_{b\mathcal{F}}) = \frac{1}{2}\delta_{ab}$, one finds $C_2(\mathcal{F}) = (N^2 - 1)/(2N)$ for the fundamental and $C_2(\mathcal{A}) = N$ for the adjoint representation [50]. This concludes the derivation of the effective NJL couplings $G_{\mathcal{F}}$ and $G_{\mathcal{A}}$ given below Eq. (2.19).

B. Gauge group averaging with continuum quarks

In this appendix we justify our prescription (2.18) for adding quarks to the lattice model of the gauge sector. In contrast to Eq. (2.18), the authors of Ref. [20] calculated the quark

thermodynamic potential Ω_q in the mean-field NJL model with a constant background gauge field and set $\langle \Omega_q \rangle_{\text{mf}}$ as the quark contribution to the thermodynamic potential.

To start, let us emphasize that any attempt at adding *continuum* quarks to a lattice gauge model is at best heuristic. For a proper treatment one would need to discretize the quark action as well, thereby losing the computational simplicity of the mean-field NJL model. With this in mind, below we provide a qualitative argument why Eq. (2.18) is a reasonable approximation.

Imagine adding quarks to the lattice model (2.1); the full action then formally reads $\mathcal{S} = \mathcal{S}_g + \bar{\psi} \mathcal{D} \psi$, where \mathcal{D} is the Dirac operator including the background gauge field the quarks interact with. The full partition function of the system is obtained as

$$\mathcal{Z} = \int dL d\psi d\bar{\psi} e^{-\mathcal{S}} = \int dL e^{-\mathcal{S}_g} \det \mathcal{D}. \quad (\text{B.1})$$

Using the same trick of introducing the Weiss mean-field action as in Sec. 2, this leads to

$$\mathcal{Z} = \left\langle e^{-(\mathcal{S}_g - \mathcal{S}_{\text{mf}})} \det \mathcal{D} \right\rangle_{\text{mf}} \int dL e^{-\mathcal{S}_{\text{mf}}}. \quad (\text{B.2})$$

This expression is still exact and includes all correlations between the gauge and the quark sectors. However, to evaluate it numerically would be very demanding. We therefore perform a mean-field approximation by setting

$$\left\langle e^{-(\mathcal{S}_g - \mathcal{S}_{\text{mf}})} \det \mathcal{D} \right\rangle_{\text{mf}} \approx e^{-\langle \mathcal{S}_g - \mathcal{S}_{\text{mf}} \rangle_{\text{mf}}} \langle \det \mathcal{D} \rangle_{\text{mf}}. \quad (\text{B.3})$$

This is equivalent to the Weiss mean-field approximation introduced in Sec. 2 plus neglecting the correlations between the gauge and quark sectors.⁵ The full thermodynamic potential is then given by the gauge part (2.9) augmented with $-T \log \langle \det \mathcal{D} \rangle_{\text{mf}}$. One can therefore see that averaging the determinant of the Dirac operator is more natural than averaging its logarithm. However, Eq. (2.18) commits one more approximation: it neglects correlations between modes of different momentum and spin. While the former is naturally incorporated in Eq. (2.18) by the momentum integral, the latter has to be imposed by hand (by adding the power 1/2 to the argument of the logarithm) in presence of a diquark condensate, since this ties together quarks of opposite spin. Somewhat ambiguous as this procedure is, it does reproduce the prescription of Abuki and Fukushima [20] when $\Delta = 0$, and, unlike other prescriptions, it leads to a thermodynamically consistent potential Ω_q as will now be discussed.

Let us start rather generally by addressing the following question: why have we used the complicated-looking Weiss mean-field approximation instead of the simple “naive” one?⁶ To find the answer it is useful to understand the relation between the two approximations. Let us write the Haar measure (2.6) as

$$dL = H(\theta) \prod_{i=1}^{N_c-1} d\theta_i. \quad (\text{B.4})$$

⁵The lack of correlations, in particular the feedback from the dense quark matter into the gauge sector, makes the usual PNJL model rather trivial in the region of cold dense matter. It would be interesting to see to what extent these correlations can be taken into account within the present model.

⁶We are indebted to Kenji Fukushima for clarifying this point at the initial stage of the project.

The group integral of a given function $f(\theta)$, weighted by the mean-field action, can then be expressed as

$$\int dL f(\theta) e^{-\mathcal{S}_{\text{mf}}} = \int \prod_{i=1}^{N_c-1} d\theta_i f(\theta) e^{-\mathcal{S}_{\text{mf}} + \log H(\theta)}. \quad (\text{B.5})$$

While in the Weiss mean-field approximation this group integral is evaluated exactly, the naive mean-field approximation can be obtained by picking the contribution of the saddle point of the ‘‘action’’ $\mathcal{S}_{\text{mf}} - \log H(\theta)$. Indeed, let the saddle point, depending on α, β , be θ_{mf} . Then the above integral is approximated by $f(\theta_{\text{mf}}) e^{-\mathcal{S}_{\text{mf}}(\theta_{\text{mf}}) + \log H(\theta_{\text{mf}})}$. The average of any function of the Polyakov loop is thus simply

$$\langle f(\theta) \rangle_{\text{mf}} = f(\theta_{\text{mf}}). \quad (\text{B.6})$$

Then, in the gauge thermodynamic potential (2.9), the Weiss mean fields α, β drop out and the result depends only on θ_{mf} ,

$$\frac{\Omega_g^{\text{naive}} a_s^3}{TV} = -2(d-1)N_c^2 e^{-a/T} \ell_{\text{F}}(\theta_{\text{mf}}) \ell_{\text{F}}^*(\theta_{\text{mf}}) - \log H(\theta_{\text{mf}}). \quad (\text{B.7})$$

In some particular cases, it can even be expressed solely in terms of the traced Polyakov loop.

Let us now for simplicity assume that the chemical potential is zero so that there is no pairing and the Polyakov loop and its complex conjugate give rise to the same expectation values. The quasiparticle contribution to the quark thermodynamic potential (2.18) with quarks in the representation \mathcal{R} of the gauge group then reads

$$-2 \int \frac{d^3 \mathbf{k}}{(2\pi)^3} \left[\epsilon_{\mathbf{k}} \dim \mathcal{R} + T \text{Tr} \log(\mathbb{1} + L_{\mathcal{R}} e^{-\epsilon_{\mathbf{k}}/T}) \right]. \quad (\text{B.8})$$

The fundamental and adjoint Polyakov loops are related by $\text{Tr} L_{\text{A}} = |\text{Tr} L_{\text{F}}|^2 - 1$, hence the same relation holds for their expectation values in the naive mean-field approximation. This means that at low temperature when the fundamental Polyakov loop goes to zero, the adjoint loop should become negative. Disregarding the obvious disagreement of this conclusion with lattice simulations, it would moreover be a disaster for the mean-field PNJL model. Indeed, at low temperatures,

$$\text{Tr} \log(\mathbb{1} + L_{\mathcal{R}} e^{-\epsilon_{\mathbf{k}}/T}) \approx e^{-\epsilon_{\mathbf{k}}/T} \text{Tr} L_{\mathcal{R}}. \quad (\text{B.9})$$

A negative value of the Polyakov loop would thus imply that the quarks would give a negative contribution to the pressure, leading to a thermodynamic instability. We conclude that the naive mean-field approximation cannot be applied to QCD with adjoint quarks.

We will now show that a similar, albeit milder, instability occurs when one defines the quark contribution to the thermodynamic potential by taking $\langle \Omega_q \rangle_{\text{mf}}$. For the sake of simplicity we focus on aQC₂D at low temperature. The mean field α is then strictly zero (deconfinement is a sharp phase transition for adjoint quarks) and the average of the quark thermodynamic potential is easily evaluated using the integrals (14) of Ref. [18]. In accord

with the general expression (2.18) (with swapped logarithm and averaging operations), one finds

$$2 \langle \log[(1+x)(1+2x \cos 2\theta + x^2)] \rangle_{\text{mf}} = 2[\log(1+x) - x], \quad (\text{B.10})$$

where $x = e^{-E_{\mathbf{k}}^c/T}$. Even though the leading term, linear in x and proportional to $\langle \text{Tr } L_A \rangle_{\text{mf}}$, now vanishes, the total quaquark pressure is still negative. This negative contribution is numerically small, yet it makes the thermodynamics in principle ill-defined.

It is easy to see that this problem does not arise when the group average is taken inside the logarithm as in Eq. (2.18). Then at low temperature when $\alpha = 0$, one gets instead of Eq. (B.10)

$$2 \log \langle (1+x)(1+2x \cos 2\theta + x^2) \rangle_{\text{mf}} = 2 \log[(1+x)(1-x+x^2)] = 2 \log(1+x^3). \quad (\text{B.11})$$

The pressure is now strictly positive and even looks like a pressure of noninteracting fermionic quasiparticles with energy $3E_{\mathbf{k}}^c$.

One comment is appropriate regarding the last claim. In the PNJL model for physical, three-color QCD with fundamental quarks, one observes the same behavior at low temperature. More precisely, the mean field α is never strictly zero at any nonzero temperature, so the quark contribution to the pressure is proportional to $\log(1+3x\ell_F + 3x^2\ell_F^* + x^3)$. At low temperature when the Polyakov loop is suppressed this reduces to $\log(1+x^3)$, which is usually interpreted as a manifestation of the fact that one needs three quarks to create a color-singlet state. This observation suggests that the PNJL model is a natural framework for a description of the quarkyonic phase in cold dense quark matter [51, 52, 53]. However, as Eq. (B.11) clearly shows, this is somewhat misleading: the same low-temperature behavior of the pressure arises in *two-color* QCD with adjoint quarks, so it does not directly reflect the number of quarks needed to construct a color singlet.

A second attempt at interpreting $\log(1+x^3)$ might be that both examples of three-color fundamental and two-color adjoint quarks are governed by the dimension of the representation. However, in two-color QCD it is easy to calculate the same quantity with quarks in higher representations, showing that there is no simple general relation between the representation and the form of the low-temperature pressure. For instance, in aQCD below the deconfinement temperature, the coefficients $\omega_{1,2,3}$ take on the values $\omega_1 = -1$, $\omega_2 = 0$, $\omega_3 = 1/8$. Consequently, the quark pressure is proportional to $2 \log(1+x^3+x^5+x^8)$.

C. Group integration for $SU(N)$

In this appendix we show that some of the group integrals can be performed for arbitrary N [54, 55]. (For the sake of legibility, we abbreviate N_c as N .) Let us define the generating function

$$\mathcal{G}(z, \bar{z}) = \left\langle \prod_{i=1}^N e^{ze^{i\theta_i}} e^{\bar{z}e^{-i\theta_i}} \right\rangle_{\text{mf}}. \quad (\text{C.1})$$

In order to calculate it, we write the mean-field action (2.5) for one lattice site as

$$\mathcal{S}_{\text{mf}} = - \sum_{i=1}^N (\alpha \cos \theta_i + i\beta \sin \theta_i). \quad (\text{C.2})$$

Furthermore, we use the fact that the Haar measure (2.6) may be written as a square of a Vandermonde determinant,

$$dL = \prod_{i=1}^N d\theta_i \delta(\theta_1 + \dots + \theta_N) \varepsilon_{i_1 \dots i_N} \varepsilon_{j_1 \dots j_N} e^{i\theta_1(i_1-j_1)} \dots e^{i\theta_N(i_N-j_N)}. \quad (\text{C.3})$$

The last trick is to express the (periodic) δ -function in terms of its Fourier series,

$$\delta(\theta_1 + \dots + \theta_N) = \frac{1}{2\pi} \sum_{m=-\infty}^{+\infty} e^{im(\theta_1 + \dots + \theta_N)}. \quad (\text{C.4})$$

The integration over the angles θ_i now completely factorizes in terms of a single master integral,

$$\mathcal{I}_n(u, v) = \frac{1}{2\pi} \int_0^{2\pi} d\theta e^{in\theta} e^{u \cos \theta + iv \sin \theta}, \quad (\text{C.5})$$

For real u and pure imaginary v , $v = iw$, which is the case if $\beta = 0$, the master integral can again be expressed with the help of the modified Bessel function,

$$\mathcal{I}_n(u, iw) = \left(\frac{u - iw}{\sqrt{u^2 + w^2}} \right)^n I_n(\sqrt{u^2 + w^2}). \quad (\text{C.6})$$

The final formula for the generating function (C.1) reads

$$\mathcal{G}(z, \bar{z}) = \frac{\sum_{m=-\infty}^{+\infty} \det \mathcal{I}_{m+i-j}(\alpha + z + \bar{z}, \beta + z - \bar{z})}{\sum_{m=-\infty}^{+\infty} \det \mathcal{I}_{m+i-j}(\alpha, \beta)}. \quad (\text{C.7})$$

Looking back at Eq. (C.1) one sees that expanding the exponentials, the Taylor coefficient of the $z^m \bar{z}^n$ term resums all eigenvalues of the Polyakov loop in the $F^m \otimes \bar{F}^n$ representation, F being the fundamental one. That is, one has

$$\langle \text{Tr } L_{F^m \otimes \bar{F}^n} \rangle_{\text{mf}} = \left. \frac{\partial^{m+n}}{\partial z^m \partial \bar{z}^n} \mathcal{G}(z, \bar{z}) \right|_{\substack{z=0 \\ \bar{z}=0}}. \quad (\text{C.8})$$

The expectation values of Polyakov loops in all *irreducible* representations can be obtained from this formula by simply observing that the (traced) Polyakov loop in a direct sum of two representations is equal to the sum of the loops in these representations.

Let us remark here that the thermodynamic potential of the three-color pure gauge theory (4.3) can be derived using the same argument, and the group integrals involved are special cases of those considered above. Indeed, the function $F(\alpha)$ (4.2) equals the denominator in Eq. (C.7) at $\beta = 0$ up to a trivial numerical prefactor. Changing this prefactor just shifts the thermodynamic potential by a constant, and noting that $F(0) = 1$, it can be fixed by demanding that $\Omega_g = 0$ for $\alpha = 0$.

A more compact formula can again be obtained for the special case of two colors. Then, we can set $\beta = 0$ and $\bar{z} = 0$. Also, $\prod_{i=1}^2 e^{ze^{i\theta}} = e^{2z \cos \theta}$. The one-dimensional group integration can be performed directly and one finds

$$\mathcal{G}(z) = \frac{I_0(2\alpha + 2z) - I_2(2\alpha + 2z)}{I_0(2\alpha) - I_2(2\alpha)} = \frac{\alpha}{\alpha + z} \frac{I_1(2\alpha + 2z)}{I_1(2\alpha)}. \quad (\text{C.9})$$

While the latter expression is more compact, the former is more convenient for taking the derivatives in order to extract the expectation values of the Polyakov loops.

Finally, let us show that even the averages (4.7) can be expressed analytically in terms of a series of modified Bessel functions [56], and thus speed up the numerical evaluation of the thermodynamic potential. Using trigonometric identities, these averages can be written as a linear combination of terms of the type

$$K_{abc}(\alpha) = \langle e^{i(a\theta_1 + b\theta_2 + c\theta_3)} \rangle_{\text{mf}}, \quad (\text{C.10})$$

where a, b, c are integers. Using the same trick of rewriting the Haar measure as a Vandermonde determinant and introducing the periodic δ -function as in Eqs. (C.3) and (C.4), this becomes

$$K_{abc}(\alpha) = \frac{1}{6F(\alpha)} \sum_{m=-\infty}^{+\infty} \sum_{i,j,k=1}^3 \varepsilon_{ijk} \begin{vmatrix} I_{m+i-1+a}(\alpha) & I_{m+i-2+a}(\alpha) & I_{m+i-3+a}(\alpha) \\ I_{m+j-1+b}(\alpha) & I_{m+j-2+b}(\alpha) & I_{m+j-3+b}(\alpha) \\ I_{m+k-1+c}(\alpha) & I_{m+k-2+c}(\alpha) & I_{m+k-3+c}(\alpha) \end{vmatrix}. \quad (\text{C.11})$$

References

- [1] M. G. Alford, A. Kapustin, and F. Wilczek, *Imaginary chemical potential and finite fermion density on the lattice*, *Phys. Rev.* **D59** (1999) 054502, [[hep-lat/9807039](#)].
- [2] D. T. Son and M. A. Stephanov, *QCD at Finite Isospin Density*, *Phys. Rev. Lett.* **86** (2001) 592–595, [[hep-ph/0005225](#)].
- [3] J. B. Kogut, M. A. Stephanov, and D. Toublan, *On two-color QCD with baryon chemical potential*, *Phys. Lett.* **B464** (1999) 183–191, [[hep-ph/9906346](#)].
- [4] J. B. Kogut, M. A. Stephanov, D. Toublan, J. J. M. Verbaarschot, and A. Zhitnitsky, *QCD-like theories at finite baryon density*, *Nucl. Phys.* **B582** (2000) 477–513, [[hep-ph/0001171](#)].
- [5] M. E. Peskin, *The alignment of the vacuum in theories of technicolor*, *Nucl. Phys.* **B175** (1980) 197–233.
- [6] J. Bijnens and J. Lu, *Technicolor and other QCD-like theories at next-to-next-to-leading order*, *J. High Energy Phys.* **11** (2009) 116, [[arXiv:0910.5424](#)].
- [7] L. A. Kondratyuk, M. M. Giannini, and M. I. Krivoruchenko, *The SU(2) colour superconductivity*, *Phys. Lett.* **B269** (1991) 139–143.
- [8] C. Ratti and W. Weise, *Thermodynamics of two-color QCD and the Nambu–Jona-Lasinio model*, *Phys. Rev.* **D70** (2004) 054013, [[hep-ph/0406159](#)].
- [9] G.-f. Sun, L. He, and P. Zhuang, *BEC-BCS crossover in the Nambu–Jona-Lasinio model of QCD*, *Phys. Rev.* **D75** (2007) 096004, [[hep-ph/0703159](#)].

- [10] T. Brauner, K. Fukushima, and Y. Hidaka, *Two-color quark matter: $U(1)_A$ restoration, superfluidity, and quarkyonic phase*, *Phys. Rev.* **D80** (2009) 074035, [[arXiv:0907.4905](#)].
- [11] J. O. Andersen and T. Brauner, *Phase diagram of two-color quark matter at nonzero baryon and isospin density*, *Phys. Rev.* **D81** (2010) 096004, [[arXiv:1001.5168](#)].
- [12] H. Nishimura and M. C. Ogilvie, *Polyakov–Nambu–Jona-Lasinio model for adjoint fermions with periodic boundary conditions*, *Phys. Rev.* **D81** (2010) 014018, [[arXiv:0911.2696](#)].
- [13] Á. Mócsy, F. Sannino, and K. Tuominen, *Confinement versus Chiral Symmetry*, *Phys. Rev. Lett.* **92** (2004) 182302, [[hep-ph/0308135](#)].
- [14] F. Sannino and K. Tuominen, *Tetracritical behavior in strongly interacting theories*, *Phys. Rev.* **D70** (2004) 034019, [[hep-ph/0403175](#)].
- [15] A. Gocksch and M. Ogilvie, *An effective strong coupling lattice model for finite temperature QCD*, *Phys. Lett.* **B141** (1984) 407–410.
- [16] A. Dumitru, Y. Hatta, J. Lenaghan, K. Orginos, and R. D. Pisarski, *Deconfining phase transition as a matrix model of renormalized Polyakov loops*, *Phys. Rev.* **D70** (2004) 034511, [[hep-th/0311223](#)].
- [17] K. Fukushima and Y. Hidaka, *Model study of the sign problem in the mean-field approximation*, *Phys. Rev.* **D75** (2007) 036002, [[hep-ph/0610323](#)].
- [18] K. Fukushima, *Relation between the Polyakov loop and the chiral order parameter at strong coupling*, *Phys. Rev.* **D68** (2003) 045004, [[hep-ph/0303225](#)].
- [19] S. Gupta, K. Hübner, and O. Kaczmarek, *Renormalized Polyakov loops in many representations*, *Phys. Rev.* **D77** (2008) 034503, [[arXiv:0711.2251](#)].
- [20] H. Abuki and K. Fukushima, *Gauge dynamics in the PNJL model: Color neutrality and Casimir scaling*, *Phys. Lett.* **B676** (2009) 57–62, [[arXiv:0901.4821](#)].
- [21] K. Fukushima, *Chiral effective model with the Polyakov loop*, *Phys. Lett.* **B591** (2004) 277–284, [[hep-ph/0310121](#)].
- [22] E. Megías, E. Ruiz Arriola, and L. L. Salcedo, *Polyakov loop in chiral quark models at finite temperature*, *Phys. Rev.* **D74** (2006) 065005, [[hep-ph/0412308](#)].
- [23] C. Ratti, M. A. Thaler, and W. Weise, *Phases of QCD: Lattice thermodynamics and a field theoretical model*, *Phys. Rev.* **D73** (2006) 014019, [[hep-ph/0506234](#)].
- [24] S. Rößner, C. Ratti, and W. Weise, *Polyakov loop, diquarks, and the two-flavor phase diagram*, *Phys. Rev.* **D75** (2007) 034007, [[hep-ph/0609281](#)].
- [25] K. Fukushima, *Phase diagrams in the three-flavor Nambu–Jona-Lasinio model with the Polyakov loop*, *Phys. Rev.* **D77** (2008) 114028, [[arXiv:0803.3318](#)].
- [26] J. B. Kogut, J. Polonyi, H. W. Wyld, and D. K. Sinclair, *Hierarchical Mass Scales in Lattice Gauge Theories with Dynamical, Light Fermions*, *Phys. Rev. Lett.* **54** (1985) 1980–1982.
- [27] F. Karsch and M. Lütgemeier, *Deconfinement and chiral symmetry restoration in an $SU(3)$ gauge theory with adjoint fermions*, *Nucl. Phys.* **B550** (1999) 449–464, [[hep-lat/9812023](#)].
- [28] J. Engels, S. Holtmann, and T. Schulze, *Scaling and Goldstone effects in a QCD with two flavours of adjoint quarks*, *Nucl. Phys.* **B724** (2005) 357–379, [[hep-lat/0505008](#)].

- [29] M. Ünsal, *Abelian Duality, Confinement, and Chiral-Symmetry Breaking in a SU(2) QCD-like Theory*, *Phys. Rev. Lett.* **100** (2008) 032005, [[arXiv:0708.1772](#)].
- [30] A. Lohwater, *Introduction to Inequalities*. Online e-book in PDF format, 1982.
- [31] H. Georgi, *Lie Algebras in Particle Physics*. Frontiers in Physics. Perseus Books, Reading, Massachusetts, second ed., 1999.
- [32] S. Hands, I. Montvay, S. Morrison, M. Oevers, L. Scorzato, and J.-I. Skullerud, *Numerical study of dense adjoint matter in two color QCD*, *Eur. Phys. J.* **C17** (2000) 285–302, [[hep-lat/0006018](#)].
- [33] K. Fukushima and K. Iida, *Larkin–Ovchinnikov–Fulde–Ferrell state in two-color quark matter*, *Phys. Rev.* **D76** (2007) 054004, [[arXiv:0705.0792](#)].
- [34] K. Splittorff, D. T. Son, and M. A. Stephanov, *QCD-like theories at finite baryon and isospin density*, *Phys. Rev.* **D64** (2001) 016003, [[hep-ph/0012274](#)].
- [35] C. Vafa and E. Witten, *Parity Conservation in Quantum Chromodynamics*, *Phys. Rev. Lett.* **53** (1984) 535–536.
- [36] M. Buballa, *NJL model analysis of quark matter at large density*, *Phys. Rep.* **407** (2005) 205–376, [[hep-ph/0402234](#)].
- [37] J. Ambjørn, P. Olesen, and C. Peterson, *Stochastic confinement and dimensional reduction: (I). Four-dimensional SU(2) lattice gauge theory*, *Nucl. Phys.* **B240** (1984) 189–212.
- [38] L. Del Debbio, M. Faber, J. Greensite, and Š. Olejník, *Casimir scaling versus Abelian dominance in QCD string formation*, *Phys. Rev.* **D53** (1996) 5891–5897, [[hep-lat/9510028](#)].
- [39] Y. Schröder, *The static potential in QCD to two loops*, *Phys. Lett.* **B447** (1999) 321–326, [[hep-ph/9812205](#)].
- [40] C. Anzai, Y. Kiyo, and Y. Sumino, *Violation of Casimir Scaling for Static QCD Potential at Three-loop Order*, [arXiv:1004.1562](#).
- [41] S. Deldar, *Static SU(3) potentials for sources in various representations*, *Phys. Rev.* **D62** (2000) 034509, [[hep-lat/9911008](#)].
- [42] G. S. Bali, *Casimir scaling of SU(3) static potentials*, *Phys. Rev.* **D62** (2000) 114503, [[hep-lat/0006022](#)].
- [43] C. Piccioni, *Casimir scaling in SU(2) lattice gauge theory*, *Phys. Rev.* **D73** (2006) 114509, [[hep-lat/0503021](#)].
- [44] V. I. Shevchenko and Y. A. Simonov, *Casimir Scaling as a Test of QCD Vacuum Models*, *Phys. Rev. Lett.* **85** (2000) 1811–1814, [[hep-ph/0001299](#)].
- [45] P. N. Meisinger, T. R. Miller, and M. C. Ogilvie, *Phenomenological equations of state for the quark-gluon plasma*, *Phys. Rev.* **D65** (2002) 034009, [[hep-ph/0108009](#)].
- [46] H.-M. Tsai and B. Müller, *Phenomenology of the three-flavor PNJL model and thermal strange quark production*, *J. Phys.* **G36** (2009) 075101, [[arXiv:0811.2216](#)].
- [47] R. N. Cahn, *Semi-Simple Lie Algebras and Their Representations*. Dover Publications, New York, 2006.
- [48] S. Hands, S. Kim, and J.-I. Skullerud, *Deconfinement in dense two-color QCD*, *Eur. Phys. J.* **C48** (2006) 193–206, [[hep-lat/0604004](#)].

- [49] S. Hands, S. Kim, and J.-I. Skullerud, *Quarkyonic phase in dense two color matter*, *Phys. Rev.* **D81** (2010) 091502, [[arXiv:1001.1682](#)].
- [50] M. E. Peskin and D. V. Schroeder, *An Introduction to Quantum Field Theory*. Addison-Wesley, Reading, Massachusetts, 1995.
- [51] L. McLerran and R. D. Pisarski, *Phases of dense quarks at large N_c* , *Nucl. Phys.* **A796** (2007) 83–100, [[arXiv:0706.2191](#)].
- [52] B.-J. Schaefer, J. M. Pawłowski, and J. Wambach, *Phase structure of the Polyakov-quark-meson model*, *Phys. Rev.* **D76** (2007) 074023, [[arXiv:0704.3234](#)].
- [53] H. Abuki, R. Anglani, R. Gatto, G. Nardulli, and M. Ruggieri, *Chiral crossover, deconfinement, and quarkyonic matter within a Nambu–Jona-Lasinio model with the Polyakov loop*, *Phys. Rev.* **D78** (2008) 034034, [[arXiv:0805.1509](#)].
- [54] M. Creutz, *On invariant integration over $SU(N)$* , *J. Math. Phys.* **19** (1978) 2043–2046.
- [55] J. B. Kogut, M. Snow, and M. Stone, *Mean field and Monte Carlo studies of $SU(N)$ chiral models in three dimensions*, *Nucl. Phys.* **B200** (1982) 211–231.
- [56] P. H. Damgaard, *The free energy of higher representation sources in lattice gauge theories*, *Phys. Lett.* **B194** (1987) 107–113.